Master's Thesis

Composition and prognostic significance of T helper lymphocytes in lung cancer

Essi Kivelä

University of Jyväskylä

Department of Biological and Environmental Science

27 March 2024

UNIVERSITY OF JYVÄSKYLÄ, Faculty of Mathematics and Science
Department of Biological and Environmental Science
Master's Degree Programme in Cell and Molecular Biology

Kivelä, Essi Composition and prognostic significance of T helper lymphocytes in lung cancer

MSci Thesis 30 p., 5 appendices (8 p.)
Supervisors: Ph. D Jari Ylänne, D. Sc. Jatta Saarenheimo and M. Sc. Hanna Elomaa
Revisors: Ph. D Jan Böhm and D. Sc. Jonna Nykky
March 2024

Keywords: adenocarcinoma, innate lymphoid cell, machine learning-based image analysis, multiplex-immunohistochemistry, NSCLC, squamous cell carcinoma, tissue microarray

Lung cancer is the most fatal cancer worldwide with non-small cell lung cancer and its subtypes adenocarcinoma and squamous cell carcinoma accounting for approximately 80% of all lung cancer cases. In lung cancer treatment immunotherapies, such as PD-L1 checkpoint inhibitors, are widely in use alongside the conventional cancer treatments surgery, radiation, and chemotherapy to improve treatment outcome and survival rate. Immune cell density and composition are heterogenous between tumors and different tumor sites, and research could help better understand the interactions between host tissue and tumor to reveal possible new targets for immunotherapy, as well as new prognostic biomarkers. Multiplex immunohistochemistry enables the use of several monoclonal antibodies for the same tissue section so that many different types of immune cells and their relations to each other to be investigated for effective biomarker research. In the thesis study different subtypes of T lymphocytes, innate lymphoid cells (ILCs), macrophages, and natural killer (NK) cells were stained using specific monoclonal antibodies to calculate respective cell densities within the central tumor and invasive margin of lung cancer tumors. $CD8^+$ and $CD4^+$ T lymphocytes, ILCs, NK cells and macrophages were phenotyped in QuPath bioimage analysis software, while regulatory T lymphocytes, T helper lymphocyte subtypes Th_1, Th_2, and Th_{17}, and ILC subtypes ILC1, ILC2, and ILC3 were phenotyped by intensity thresholds. Density calculations for each cell type within the tumor center and invasive margin were made. Together with extensive patient data the effect of Th_1, Th_2, and Th_{17} on long-term survival was assessed. Th_{17} was found to have a statistically significant impact on cancer-specific survival three years post operation in the tumor center, and five years post operation both in the tumor center and invasive margin. The findings are, however, contradictory to most results in literature, and more research needs to be made to specify why such results were obtained.

JYVÄSKYLÄN YLIOPISTO, Matemaattis-luonnontieteellinen tiedekunta
Bio- ja ympäristötieteiden laitos
Solu- ja molekyylibiologian maisteriohjelma
Kivelä, Essi

Auttaja T-lymfosyyttien koostumus ja prognostinen merkitys keuhkosyövässä

Pro gradu tutkielma: 30 s., 5 liitettä (8 s.)
Työn ohjaajat: Prof. Jari Ylänne, FT Jatta Saarenheimo ja FM Hanna Elomaa
Tarkastajat: FT Jan Böhm ja FT Jonna Nykky
Maaliskuu 2024

Hakusanat: adenokarsinooma, ei-pienisoluinen keuhkosyöpä, immunohistokemia, levyepiteelikarsinooma, monikudosblokki, synnynnäinen lymfoidisolu

Maailmanlaajuisesti keuhkosyöpä on kuolettavin kaikista syövistä. Ei-pienisoluinen keuhkosyöpä ja sen alatyypit adeno- ja levyepiteelikarsinooma kattavat noin 80 % kaikista keuhkosyöpätapauksista. Immunoterapiaa, kuten PD-L1 inhibiittoreita, käytetään jo keuhkosyövän hoidossa yhdessä perinteisten hoitomuotojen, kuten leikkauksen, säteilyhoidon ja kemoterapian, kanssa, jolloin hoito on tehokkaampaa ja suhteellinen elossaololuku nousee. Immuunisolujen sijainti ja määrä voi vaihdella suuresti kasvaimen eri alueiden ja potilaiden välillä. Näiden eroavaisuuksien ja keskinäisen vuorovaikutuksen ymmärtäminen auttaa löytämään ja tunnistamaan uusia immunoterapiakohteita sekä prognostisia biomarkkereita. Useiden eri immuunisolujen ja niiden keskinäisten suhteiden tutkiminen on mahdollista syklisen multiplex immunohistokemiallisen värjäysmenetelmän avulla. Syklinen värjäysmenetelmä mahdollistaa jokaisen solun tunnistamisen ja luokittelun usean markkerin avulla samanaikaisesti. Lisäksi solujen välisiä spatiaalisia suhteita ja solutiheyksiä voidaan mitata ja laskea tietokoneavusteisesti. Tutkimuksessa tutkittiin T lymfosyyttejä, luonnollisia lymfosyyttejä (engl. innate lymphoid cell, ILC), makrofageja sekä luontaisia tappajasoluja (engl. natural killer cells, NK cells), jotka värjättiin spesifeillä monoklonaalisilla vasta-aineilla, ja niiden tiheydet keuhkokasvaimen keskellä ja invaasiorintamalla laskettiin. $CD8^+$ ja $CD4^+$ lymfosyytit, ILC ja NK solut sekä makrofagit tunnistettiin QuPath kuva-analyysiohjelmistolla. Solut luokiteltiin alatyyppeihin (säätelevät T lymfosyytit, T-auttajasolujen alatyypit Th_1, Th_2 ja Th_{17}, sekä ILC1, ILC2 ja ILC3 solut) intensiteettiraja-arvojen perusteella. Eri T lymfosyyttityyppien, ILC solujen, makrofagien, ja NK solujen solutiheydet kasvaimen keskustassa ja invaasiorintamassa laskettiin. Th_1, Th_2 ja Th_{17} solujen vaikutusta potilaiden pitkäaikaiseen selviytymiseen tutkittiin. Tilastollisesti merkittävä vaikutus syöpäspesifiin selviytymiseen kolme vuotta leikkauksen jälkeen saatiin Th_{17} solujen runsaasta esiintymisestä kasvaimen keskustassa, ja viisi vuotta leikkauksen jälkeen sekä kasvaimen keskustassa että invaasiorintamalla. Tulokset ovat ristiriidassa useimpien julkaisujen kanssa, joten lisää tutkimusta tarvitaan tulosten selittämiseksi.

TABLE OF CONTENTS

TERMS AND ABBREVIATIONS

Terms

Immunohistochemistry	A laboratory method for targeting cell surface antigens with antibodies
Invasive margin	The region on the border of healthy tissue and malignant tumor tissue
Tumor microenvironment	The environment around the tumor, including the stroma, immune cells, blood vessels, tumor cells and the extracellular matrix

Abbreviations

CT	tumor center
FOXP3	Forkhead box P3
H&E	hematoxylin and eosin
IL	interleukin
ILC	innate lymphoid cell
IM	invasive margin
INF-γ	interferon-gamma
mIHC	multiplex immunohistochemistry
NK	natural killer cell
NSCLC	non-small cell lung cancer
PD-1	Programmed cell death protein 1
PD-L1	Programmed cell death ligand 1
RORC	Retinoic acid-related orphan receptor γt
T-BET	T-box expressed in T cells
TMA	tissue microarray
TME	tumor microenvironment
TNM	tumor-node-metastasis

1 INTRODUCTION

Receiving a cancer diagnosis is a crushing feeling. Cancers had long been close to synonymous with death before modern medical developments and alternative, effective treatment methods have brought hope for a better prognosis. For decades lung cancer has been, and continues to be, the most fatal of all cancers (Sung et al. 2021). In 2020 GLOBOCAN listed over 2,2 million cases of lung cancer and almost 1,8 million deaths worldwide.

Surgery is considered the only curing treatment for lung cancer. The success of the surgery mainly depends on the patient's health and stage of the cancer. The stage is classified by the tumor-node-metastasis (TNM) system, which gives information of the size and extent of spread of the cancer and helps doctors in treatment planning. In the TNM system the T is categorized into four stages and describes the extent of the primary tumor. The N stands for lymph node involvement, and M for metastatic spread of the cancer (Detterbeck et al. 2017). In later stages the cancer has spread and sent metastases to the liver, breasts, lymph nodes, or brain, which makes treatment difficult and the prognosis significantly worse (Riihimäki et al. 2014). Therefore, early diagnosis is critically important for successful lung cancer treatment. The first symptoms of cough and shortness of breath are unfortunately often disregarded, and diagnosis and treatment are delayed until the cancer has reached an advanced stage (Nooreldeen and Bach 2021).

While surgery, chemotherapy and radiation are the primary forms of lung cancer treatment, immunotherapies have raised into significant importance (Wang et al. 2021). Contrary to conventional cancer treatments, which directly eliminate cancer cells, immunotherapies enhance the antitumor immune response of host innate and adaptive immune cells. Immunotherapies can be used together with conventional cancer treatments to enhance the treatment efficacy (Herbst et al. 2018). One of commonly used immune checkpoint inhibitors is the PD-L1 inhibitor that blocks the binding of the programmed cell death ligand 1 (PD-L1) to the receptor programmed cell death protein 1 (PD-1) present on several immune cells, such as $CD8^+$ T lymphocytes (Jain et al. 2019, Sharma et al. 2021). PD-1/PD-L1 naturally acts as a safety mechanism that protects the self from getting attacked by $CD8^+$ T lymphocytes, but the binding of PD-L1 also suppresses the immunological activity and prevents $CD8^+$ T lymphocytes from attacking cancerous cells (Syn et al. 2017). Cancer cells can prevent the breakdown of PD-L1, or they start producing it themselves to present in great quantities to the $CD8^+$ T lymphocytes and thus evade destruction by $CD8^+$ T lymphocytes (Cha et al. 2019). The pharmaceutical checkpoint inhibitor can restore the activity of the T lymphocytes by binding to PD-L1 and preventing it from binding to the PD-1 receptor (Alsaab et al. 2017). Other types of immunological medicines are actively sought for and the demand for more research is high.

1.1 Non-small cell lung cancer

Lung cancer is divided into several histological subtypes. The two main subtypes are small cell and non-small cell lung cancer (NSCLC) (Zappa and Mousa 2016). Small cell lung cancer is much less prevalent of the two with 15-20% of diagnosed lung cancer cases. Small cell lung cancer is very aggressive, and the prognosis is worse compared to NSCLC as treatment possibilities are limited (Chauhan and Liu 2020). The majority of lung cancer cases are NSCLC, which can be further categorized into its main subtypes adenocarcinoma, squamous cell carcinoma and large cell carcinoma (Zappa and Mousa 2016). Several treatment methods are available depending on the type and stage of the cancer (Herbst et al. 2018).

1.1.1 Adenocarcinoma

Adenocarcinoma accounts for around 40% of lung cancer cases (Zappa and Mousa 2016). Adenocarcinoma forms in mucus secreting cells and is typically found in the periphery of the lungs (Lappi-Blanco Sequeiros et al. 2021). Therefore, mucus secretion is a common symptom. There are multiple different subtypes of adenocarcinoma and forms in which adenocarcinoma can grow in the lung. Cancer cells can grow along the alveolar walls, form islets in mucus, or grow as a solid tumor within the lung. The growth can be described as lepidic, acinar, papillary, or solid (Lappi-Blanco Sequeiros et al. 2021). Especially papillary and micropapillary adenocarcinomas are aggressive and have a poorer prognosis compared to other adenocarcinoma types (Mali 2013). Although smoking and previous smoking greatly increase lung cancer risk, adenocarcinoma is the most common form of lung cancer in non-smoking patients (Rivera and Wakelee 2016).

1.1.2 Squamous cell carcinoma

Squamous cell carcinoma appears in the bronchi of the lungs, developing from the squamous lining of the bronchial epithelium (Lappi-Blanco Sequeiros et al. 2021). It is strongly associated with smoking (Khuder et al. 1998). Squamous cell carcinoma develops slowly and typically sends metastases only at later stages of the cancer, which gives a wider time margin for diagnosis and timely treatment when compared to adenocarcinoma (Lappi-Blanco Sequeiros et al. 2021). The prevalence of squamous cell carcinoma cases has been decreasing over the past years, probably due to a decrease in tobacco smoking (Meza et al. 2015, Liu et al. 2023).

1.2 Tumor microenvironment

The tumor microenvironment (TME) is a highly dynamic environment composed of host immune and stromal cells surrounding the tumor, the extracellular matrix, blood vessels, and the tumor cells (Albini et al. 2010, Anderson and Simon

2020). Cancer cells are capable of detaching from the controlled cell cycle and begin unrestricted division due to mutations in growth suppressor genes and growth-enhancing oncogenes, which makes the TME a critical part of cancer-body interactions (Diaz-Moralli et al. 2013). The TME lies by the controlled body and the uncontrolled tumor and mediates signaling and communication - or lack thereof - between the two. That is why studying the TME can reveal new approaches to cancer treatment as by understanding the mechanisms new ways of surpassing the tumor's defense may be found (Sounni and Noel 2013).

The tumor immune microenvironment consists of immune cells of the innate and adaptive immune systems such as T and B lymphocytes, macrophages, neutrophils, dendrite cells, and natural killer cells (Anderson and Simon 2020). The amount and composition of immune cells varies greatly between patients and even within the tumor itself, with differing immune cell compositions found in the tumor center (CT) and the invasive margin (IM) (Hu et al. 2021). The immune system has the ability to fight cancer cells, but cancer cells are capable of developing strategies to silence the immune defense and thus avoid destruction (Hanahan and Weinberg 2011, Chen and Mellman 2013).

T lymphocytes originate from the thymus and are a critical part of the adaptive immunity system (Cano and Lopera 2013). They are divided into cytotoxic $CD8^+$ T lymphocytes and $CD4^+$ T helper lymphocytes, the latter of which can be further categorized into subclasses such as regulatory T lymphocytes, Th_1, Th_2, and Th_{17} lymphocytes (Mosmann et al. 1986, Harrington et al. 2005, Sharma et al. 2021). These subtypes have targeted functions in the immune defense against antigens, and their functions correlate with those of innate lymphoid cell subtypes (Cano and Lopera 2013, de Boer et al. 2020). In relation to cancer Th_1 possesses the most potential in anti-tumor activity by secreting the cytokine interferon gamma (IFN-γ), whilst Th_{17} appears as a contradicting immune cell that can have either protumor or anti-tumor effects depending on the tumor type (Chang 2019). Th_{17} also has the capability to transform into Th_1 or regulatory T lymphocyte phenotypes, thus performing either anti-tumor (Th_1) or protumor (regulatory) functions (Ye et al. 2011).

Macrophages are a type of phagocyte, meaning they are immune cells that recognize, ingest, and destroy foreign particles such as bacteria and dying or harmful cells. In the lung macrophages have an important task in keeping the alveoli clear of debris and other harmful matter (Bowden 1984). There are two types of macrophages, M1 and M2, each of which have distinct, opposing functions in cancer immunity (Italiani and Boraschi 2014, Kalinski and Basse 2019). Overall, macrophages can be either anti-tumor (M1) or protumor (M2), or proinflammatory or anti-inflammatory, respectively, depending on the conditions. For cancer therapy ways of promoting anti-tumor M1 macrophages in the TME need to be found (Yang and Zhang 2017, Anderson et al. 2021).

Natural killer (NK) cells are lymphoid cells that are part of the innate immunity and share a common progenitor with innate lymphoid cells (Klose et al. 2014, Zhou et al. 2020). They have an effective way of directly recognizing and destroying foreign and harmful cells in a similar manner as activated $CD8^+$ T

lymphocytes by secreting cytotoxic molecules perforin and granzymes (Klose et al. 2014).

Anti-tumor cells are cells of the immune system that create an immune response against malignant tumor cells (Kalinski and Basse 2019). $CD4^+$ T lymphocytes are important regulators of other T lymphocytes. $CD4^+$ T lymphocytes secrete cytokines that activate both B lymphocytes and $CD8^+$ T lymphocytes, but also suppress the immune response against antigens (Cano and Lopera 2013). Activated $CD8^+$ T lymphocytes are effector cells that are specific to the major histocompatibility complex 1 (MHC I) receptor present on all nucleated cells (Gray et al. 2018). When they recognize their target cells they release cytotoxic molecules, perforin and granzymes, and can effectively and directly destroy cancer cells (Cano and Lopera 2013). Several research papers have found that a high expression of $CD4^+$ and $CD8^+$ T lymphocytes is correlated with a better prognosis and higher survival rate in cancer (Nedergaard et al. 2007, Fridman et al. 2011, Fridman et al. 2012).

Tumor growth promoting factors are cells or proteins in the TME that suppress the anti-tumor immune response (Kalinski and Basse 2019). Regulatory T lymphocytes are recognized by the expression of the transcription factor forkhead box P3 (FOXP3). They are cells that regulate the immune response and are critically important in self-tolerance (Cano and Lopera 2013). On the downside, regulatory T lymphocytes suppress the activity of $CD4^+$ and $CD8^+$ T lymphocytes, as does the checkpoint receptor PD-1 (Gou et al. 2020). High expression of regulatory T lymphocytes is an indication for a poorer prognosis in NSCLC as well as other cancer types (Triulzi et al. 2012, Zeng et al. 2013).

There is still more research to be done on the immune infiltration of the tumor microenvironment in lung cancer. Research that has been done has primarily focused on $CD8^+$ T lymphocytes and their role in cancer is well established, but the topic is interesting and current as immunological treatments are becoming more prevalent and their clinical significance is rising, because new treatment methods may be developed following new findings and understanding. Cancer medicines can be developed by targeting treatment strategies at points where the immune defense has been silenced (Sharma et al. 2021). This way the body's own immune system can be allowed to fight cancer cells. The plentiful presence of anti-tumor cells in the tumor microenvironment has mainly been associated with a better prognosis in several cancers (Stabile et al. 2017, Wouters and Nelson 2018, van der Leun et al. 2020). It cannot be discarded, however, that immune cell compositions have little meaning in survival if the cancer has reached an extensive stage according to the TNM system.

1.3 Innate lymphoid cells

Innate lymphoid cells (ILCs) are immune cells of the innate immune system that can be regarded the innate counterparts of T lymphocytes in terms of function (McFarland et al. 2021). They take part in upkeeping homeostasis and in several

infections and infectious diseases in addition to responding to pathogens and antigens in the body (Vivier et al. 2018). ILCs are tissue resident cells that are mostly found in soft tissues in areas that are in direct contact with pathogens, such as the skin, the respiratory and digestive tracts, and several internal organs (Spits and Cupedo 2012). Immunity can be divided into three types by the cytokines secreted by ILCs (Annunziato, Romagnani and Romagnani 2014). The role of ILCs in cancer immune defense is still widely unclear and calls for more research, but the lack of a specific ILC marker makes it a challenge (de Boer et al. 2020). As T lymphocytes are well researched and their role in several cancers has, for the most part, reached a common consensus, ILCs occupy a potential niche of undiscovered clinical significance (Eberl et al. 2015).

Type 1 (ILC-1) encompasses natural killer cells (NK) and ILC1 cells. Both cell types secrete IFN-γ and lymphotoxin-alpha (LT-α), and NK also secretes perforin and granzymes (Annunziato et al. 2014, Klose et al. 2014). IFN-γ and LT-α are central cytokines in anti-tumor immune defense due to their ability to destroy cancerous cells (Browning et al. 1996, Schroder et al. 2004). Other than anti-tumor activity type 1 functions in antiviral and antibacterial immune defense (Romagnani 1994). ILC1 closely resembles Th_1, and NK resembles $CD8^+$ T lymphocytes, in terms of function. ILC1, NK and Th_1 cells can be recognized by the marker T-box expressed in T cells (T-BET) (Annunziato et al. 2014).

Type 2 (ILC-2) cells function mainly against parasites, but they are also included in allergic reactions, and can be compared to the function of Th_2 cells (Romagnani 1994). In addition, ILC-2 can control cell metabolism. Type 2 cells secrete interleukins IL-4, IL-5, IL-8, and IL-13 as well as amphiregulin, and they express the transcription factor GATA-3 (Annunziato et al. 2014).

Type 3 (ILC-3) cells take part in defense against bacterial and fungal infections and lymphoid tissue repair. All ILC types can be found in lung tissue, but ILC-3 seems to be the predominant immune type in lung tissue, at least in certain conditions (De Grove et al. 2016, Ardain et al. 2019). Cytokines secreted by ILC-3 include IL-17a, IL-22, and IFN-γ. As the other types, also type 3 cells have a counterpart in the T helper lymphocytes, the Th_{17} cells. ILC3 and Th_{17} express retinoic acid-related orphan receptor γt (RORC) (Annunziato et al. 2014).

1.4 Immunohistochemical staining

In diagnostics special immunohistochemical (IHC) stains are used in specific cancer type determination (Leong and Wright 1987). Receptors that are specific to a certain cell are found on several individual cell types, which makes it possible to stain the desired cells by using antibodies specific to them (Ramos-Vara 2017). The most restricting factor in conventional IHC staining is the possibility to stain only a few biomarkers at a time, which may limit the extent of diagnostics if there is only a limited amount of sample material available (Tan et al. 2020). The time and cost also increase by each required stain.

1.4.1 Multiplex immunohistochemistry

Multiplex immunohistochemistry (mIHC) staining assay allows several markers to be detected from a single tissue section by consecutive staining cycles with different primary antibodies, which is useful when a larger entirety of cell types is being investigated. It is also especially beneficial in cases where sample material is limited or it needs to be conserved, and the amount of time and money spent can be reduced (Tan et al. 2020). mIHC also enables cell phenotyping by multiple markers, which is needed for cell types that cannot be accurately phenotyped by one marker only. Additionally, from mIHC images different cell type relations, such as respective distances and spatial distribution, can be examined (Zheng et al. 2020). mIHC is a relatively new technique and not yet commonly used in Finland. It is only used for research purposes but is currently gaining more and more interest due to its advantages and versatile purposes. mIHC is often combined with the usage of tissue microarray (TMA) blocks, which further enhances the economic advantages (Tsujikawa et al. 2017, Zheng et al. 2020).

mIHC differs from conventional IHC in several aspects. The 2,2'-Diaminobenzidine (DAB) chromogen commonly used in conventional IHC has been replaced by the alcohol-soluble 2-Amino-9-Ethylcarbazole (AEC) in mIHC. Between staining cycles, the antibodies are denatured and detached from the sample by heating, and after each staining cycle the slide is de-stained with ethanol. The slide is then covered using a water-soluble mounting medium for scanning. The scanned images can be constructed into one multi-layered image and converted into a pseudo-immunofluorescence image, where each marker is visualized with one color, by digitally placing them on top of each other.

While the advantages of multiplex staining are evident, there are limitations due to the repetitive heating and washing of the sample. The process is also physically harming the tissue as for scanning the slide is covered with a cover glass, which can cause tears, scratches, or bubbles on the sample. Therefore, the cycle sequence in terms of the used markers must be planned carefully. Antibodies to receptors that are known to be heat sensitive are best put in the first cycles of the staining program (Hofman et al. 2019). The most important markers for the research should preferably be placed in the earlier cycles as well so that the sample is in the best condition possible.

1.5 Tissue microarray applicability and preparation

TMA construction was first introduced by Kononen et al. in 1998. TMAs consist of several cylindrical core samples, usually 0.6–2.0 mm in diameter, punched from standard formalin-fixed paraffin-embedded tissue sample blocks to allow multiple different samples to be examined in a single block and thus speed up research while saving costs and sample material (Kallioniemi et al. 2001). However, it can be problematic to target the clinically significant feature of the sample if it is small and cannot be identified accurately by eye (Eskaros et al. 2017). There has also been debate whether a TMA block can provide a

comprehensive and representative overview of the sample as some tissues are very heterogenic in their cellular composition (Nocito et al. 2001). Several studies have debunked these worries and showed that TMAs represent the whole tissue up to a clinical standard and correlate well with previous literature (Kononen et al. 1998, Schraml 1999, Bubendorf et al. 2001, Nocito et al. 2001). It has been shown that a larger core diameter increases the accuracy and reliability of analysis as more material is included and small targets are easier to successfully include in the TMA block (Eskaros et al. 2017). It is also beneficial that more than one core sample be taken to better reflect the heterogeneity of the donor tissue sample (Kallioniemi et al. 2001). Despite the limitations TMAs are widely used for their advantages and convenience. The costs of immunohistochemical staining are reduced, tissue material is conserved, and staining variation between different samples can be minimized by using TMAs (Bubendorf et al. 2001).

TMA preparation begins with sample collection. The sample slides and blocks are collected and examined to ensure their suitability for TMA research. In cancer research the tumor must be in a viable state with active cancerous material and there must be enough tumor in the sample to get a couple core samples, preferably from different areas of the tumor, to ensure representativity. If an automated machine is used, the core sample places are marked on digitized slide images and cores are punched out of the donor block and placed into a pre-prepared recipient TMA block. Cores can also be punched out by hand using a trocar tool. The TMA block is then gently heated to soften the paraffin and attach the cores firmly into the block. After this the TMA block is ready to be trimmed and sectioned, and slides can be made for staining (Figure 1).

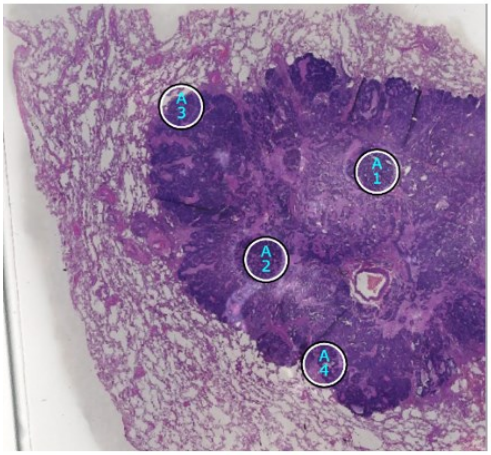

Tumor core sample areas are marked on the histology slide image.

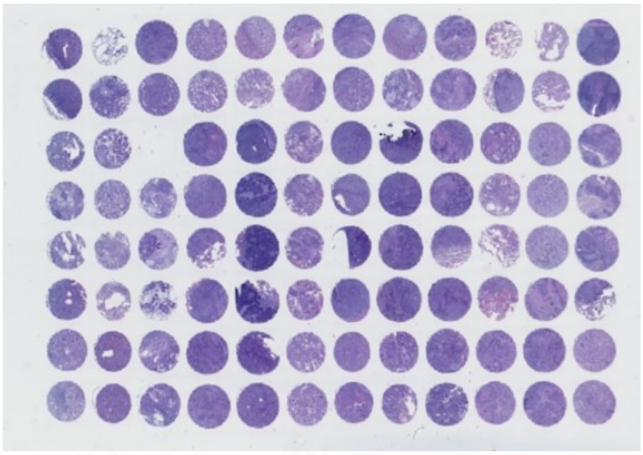

The finished TMA slide with several core samples from different tumor blocks.

Figure 1: TMA slide preparation. Core biopsy samples are taken from the donor paraffin block according to the desired tumor area marked on the corresponding digitized histology slide image. Using a drilling tool, core samples are placed into the recipient TMA block. The finished TMA block is cut using a microtome and a thin sample slice is placed on a glass slide. The finished TMA sample slide is ready to be stained.

In this study, TMA specimens consisting of NSCLC tumor samples were constructed and used for extensive immunohistochemical analysis. The aims of the experiment were to investigate the differences in immune cell densities in the tumor center and the invasive margin, and to analyze how the differences in immune cell composition affect long term survival of the patients. It was also in our interest to assess the role of T lymphocyte subtypes and ILCs in lung cancer; are there correlations in T lymphocyte subtype and ILC compositions in the tumor center and the invasive margin and the patients' survival rates? We expected that representative TMA specimens could be made with correctly punched core samples. Multiplex staining was well suited for comprehensive research of immune cell compositions as it allowed for simultaneous examination of several immune cell types and samples, which is useful with large sample pools in population-based studies. Hypothetically, higher densities of anti-tumor cells should correlate with better survival rates. We also expected to see mostly Th_1 and ILC-1 in well-recovered patients due to their anti-tumor capabilities. Immune cell research in cancer is important to better understand the mechanisms of cancer and immune system interactions; revelations may lead to new treatment possibilities and better life expectancies in cancer.

2 MATERIALS AND METHODS

The study cohort included tumor samples of 244 NSCLC adenocarcinoma and squamous cell carcinoma patients, of which 196 were included for analyses. The cohort included patients from both Central Finland healthcare district and Vaasa healthcare district. The patients underwent resection for lung cancer at Central Finland Central Hospital during 2013–2019.

2.1 Preparation of tissue microarray specimens

The most representative tumor sample with an adequate amount of viable tumor tissue was selected for TMA block construction from each patient. The hematoxylin and eosin (H&E) stained slides of the chosen tumor blocks were scanned using a digital slide scanner (NanoZoomer XR, Hamamatsu) with 20x magnification and the tumor core sites were annotated on the digital images using the TMA Slide viewer software (3DHistech). Four 1.5 mm diameter tissue core samples were taken with the TMA Master II (3DHistech) from most tumors: two from the CT and two from the IM. The invasive margin cores were targeted to span 750 µm into healthy tissue and 750 µm into the tumor. Necrotic areas, blood vessels, cartilage and other non-tumor areas were avoided. In cases of limited amount of viable tumor tissue, three core samples were taken: one from the CT and two from the IM. In total nine TMA blocks were constructed with 96 cores each (8x12). Two tonsil tissue cores were added to each TMA block as positive staining controls.

2.2 Multiplex immunohistochemistry

For immunohistochemistry staining, the TMA specimens were cut with 3.5 µm thickness. A 12-plex immunohistochemistry panel was designed to identify cytotoxic, helper, and regulatory T lymphocytes, ILCs, macrophages, NK cells, and tumor cells. The suitable antibodies with the appropriate dilutions were tested using conventional immunohistochemistry staining for a test TMA specimen consisting of tonsil, healthy lung tissue, and cancerous lung tissue. Immunohistochemistry staining was conducted with Bond-III automated IHC stainer (Leica biosystems). After optimizing the antibody dilutions, the mIHC panel was tested on a test TMA slide. All markers of the 12-plex immunohistochemistry panel in the staining order are represented in Table 1. After each staining cycle, the slides were coverslipped for scanning using a water-soluble mounting medium (VectaMount AQ Aqueuous Mounting Medium, H-5501, Vector Laboratories). The slides were scanned with 20x magnification, and afterwards the cover slides were soaked off in water. Before the following staining cycle, the slides were heated to remove the primary and secondary antibodies, and de-stained in a rising ethanol series to wash away the AEC chromogen. The staining protocol is presented in detail in Appendix 1A and Appendix 1B. The selected monoclonal antibodies along with their dilutions and antigen retrieval conditions are listed in Appendix 2.

TABLE 1: The multiplex staining program cycle sequence, the used markers, and final dilutions.

Cycle	Marker	Dilution	Target cell
1	CD8	RTU*	Cytotoxic T cell
Stain removal by hand and scanning for hematoxylin only			
2	CD3	RTU*	T cell
3	CD4	1:50	Helper T cell
4	FOXP3	1:100	Regulatory T cell
5	CD127	1:100	ILC
6	T-BET	1:400	ILC1, Th_1
7	GATA3	1:100	ILC2, Th_2
8	RORC	1:25	ILC3, Th_{17}
9	CD56	1:100	NK/NKT
10	CD68	1:40 000	Macrophage
11	CD163	1:100	Macrophage (M2)
12	KRT	1:400	Epithelium
Stain removal by hand and scanning for hematoxylin only			

* Ready to use.

2.3 Image analysis

QuPath bioimage analysis software (version 0.2.3) and Fiji ImageJ software were used for image analysis. Using the *TMA dearrayer* function in QuPath, all individual cores of the TMA blocks were identified and separated into single core images. All cores that were detached, folded, included minimal amount of tumor, or were necrotic were excluded. Each individual core image of 12 staining cycles was co-registered into one 14-channel (12 channels with primary antibodies, two channels with hematoxylin staining) pseudo-immunofluorescence image in Fiji ImageJ. The two hematoxylin channels were used for aligning nuclei of single core images. Pseudo-immunofluorescence images contained a unique color for each marker.

Pseudo-immunofluorescence images were further processed in QuPath. Two identical training images were constructed by selecting 23 tumor regions (size 40x40 µm) from randomly selected pseudo-immunofluorescence core images. The first training image was used for detecting and phenotyping cells and another training image was used to phenotype tissue compartments using a computer-assisted image analysis. Tissue compartments were categorized into tumor epithelium and stroma using a *pixel classifier*-function. Empty areas without any tissue and necrotic areas were ignored from analysis.

For the detected cells Haralick and smoothed features were calculated. Cells were then phenotyped into six classes: 1) cancer cells, KRT^+. 2) cytotoxic T lymphocytes, $CD3^+$ $CD8^+$. 3) T helper lymphocytes, $CD3^+$ $CD4^+$. 4) macrophages, $CD68^+$. 5) ILCs, $CD127^+$ $CD3^-$ $CD56^-$ $CD68^-$. 6) NK/NKT cells, $CD56^+$ $CD3^+$. The remaining cells were left uncategorized. In the training image, using an *object classifier* function, small annotations were made to phenotype the cells as one of the six classes. Cell phenotyping was continued until the automated cell recognition in QuPath could detect individual cells and categorize them into correct classes according to the made training annotations (Figure 2).

A)

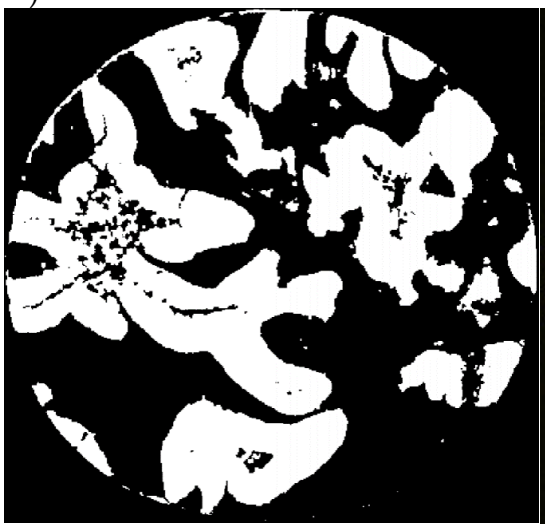

B)

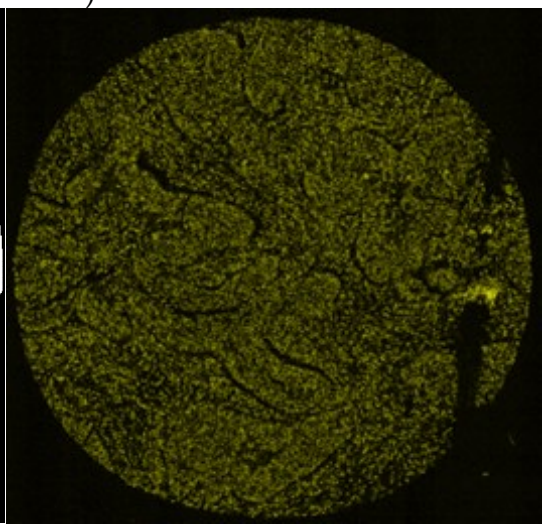

C)

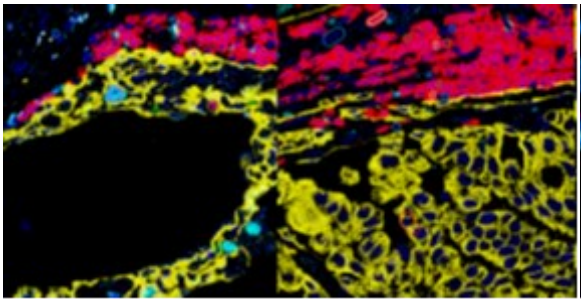

D)

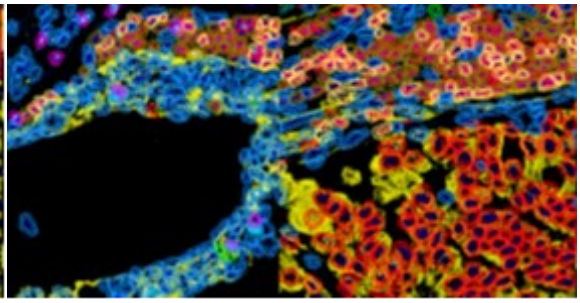

E)

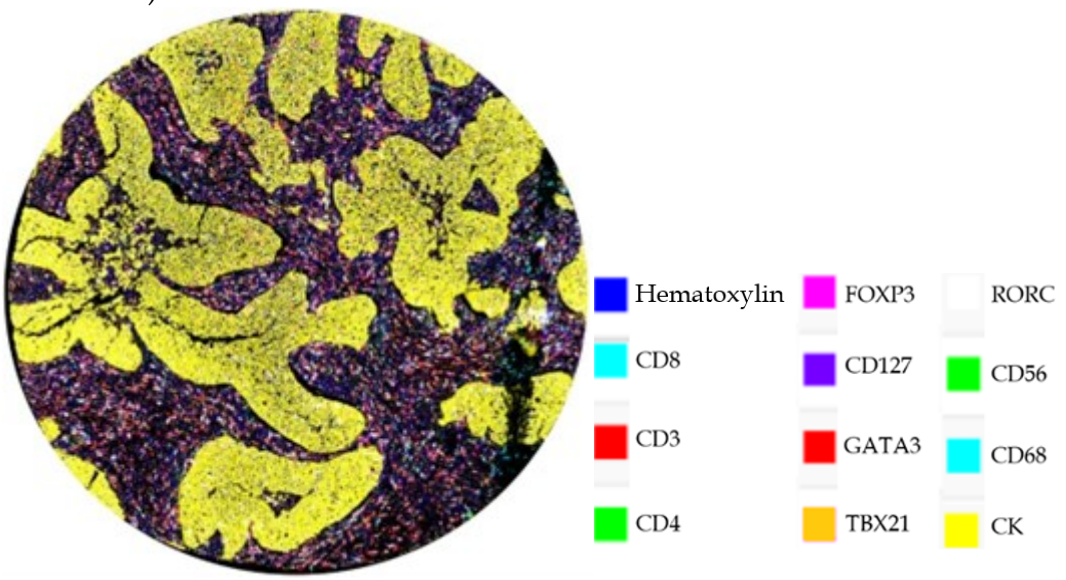
Hematoxylin
FOXP3
RORC
CD8
CD127
CD56
CD3
GATA3
CD68
CD4
TBX21
CK

Figure 2: Tissue and cell phenotyping in QuPath. A) During tissue phenotyping in QuPath tumor epithelium and stroma are identified from core images. Tumor epithelium is seen as white and stroma as black. B) A 14-channel pseudo-immunofluorescence image created in Fiji ImageJ to be used in tissue and cell phenotyping. C) In cell phenotyping small annotations were made on specific cells to assign them into the classes of interest. Cytokeratin is seen as yellow, T lymphocytes as red and macrophages as turquoise in the image. Cell nuclei appear dark blue. D) Cell phenotyping when complete. Individual cells are recognized, separated and phenotyped into the chosen classes of interest. E) The finished multiplex core image (same as A and B) where each marker is represented by a color of choice.

After image analysis in QuPath scripts based on image data were created for tissue and cell analysis. The workflow from tissue and cell classification to script creation for further analysis is presented in Figure 3.

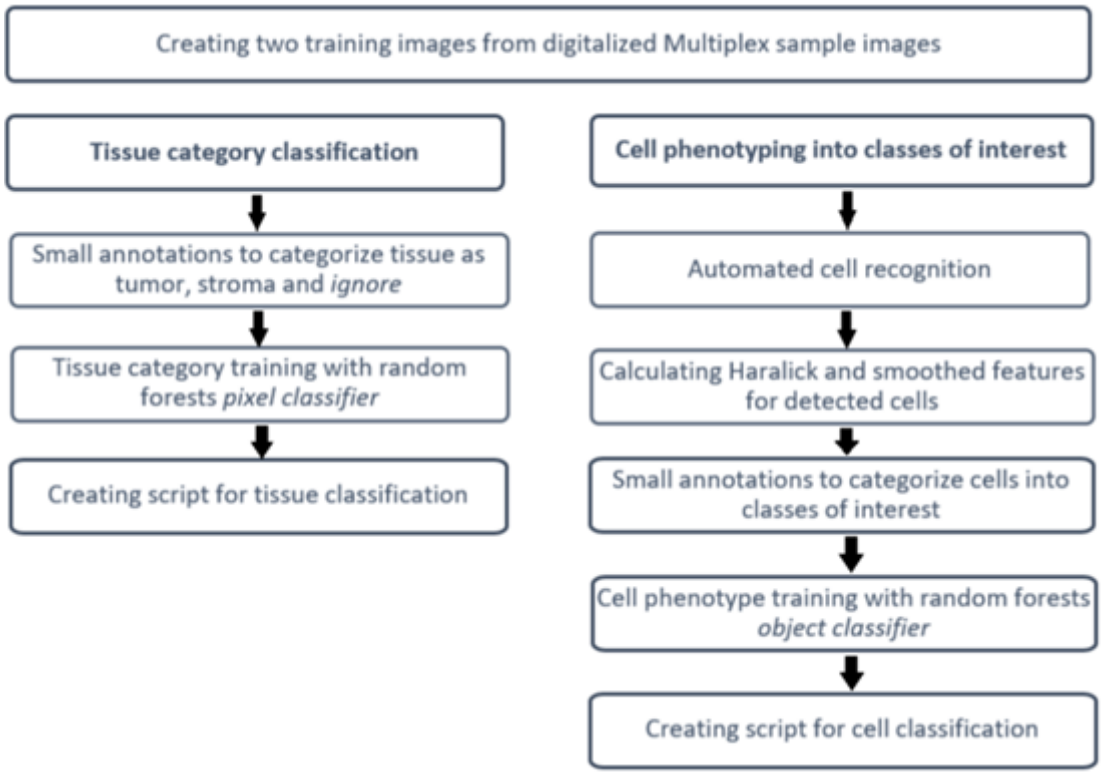

Figure 3: The workflow in QuPath to classify tissue and cells into desired groups and creating scripts for further analysis.

The created scripts were run for all multiplex cores. The cell and tissue level data were further processed in RStudio (version 1.3.1093) and R statistical programming (version 4.0.3, R Core Team). In R cell phenotyping by intensity

thresholds was made for regulatory T lymphocytes ($FOXP3^+$ T helper lymphocytes), T helper lymphocyte subtypes Th_1 ($T\text{-}BET^+$ T helper lymphocyte) Th_2 ($GATA3^+$ T helper lymphocyte) and Th_{17} ($RORC^+$ T helper lymphocyte), and ILC type 1 ($T\text{-}BET^+$ ILC), type 2 ($GATA3^+$ ILC) and type 3 ($RORC^+$ ILC) by using intensity curves shown in Appendix 3 to get all phenotyped cell categories required (Table 2).

TABLE 2: All immune cell categories in the thesis project.

Immune cell	Markers
T lymphocytes	
Cytotoxic	$CD3^+$ $CD8^+$
Helper	$CD3^+$ $CD4^+$
Regulatory*	$CD3^+$ $CD4^+$ $FOXP3^+$
Th_1*	$CD3^+$ $CD4^+$ $T\text{-}BET^+$
Th_2*	$CD3^+$ $CD4^+$ $GATA3^+$
Th_{17}*	$CD3^+$ $CD4^+$ $RORC^+$
ILCs	
ILC1*	$CD127^+$ $CD3^-$ $CD56^-$ $CD68^-$ $T\text{-}BET^+$
ILC2*	$CD127^+$ $CD3^-$ $CD56^-$ $CD68^-$ $GATA3^+$
ILC3*	$CD127^+$ $CD3^-$ $CD56^-$ $CD68^-$ $RORC^+$
Other	
NK/NKT	$CD56^+$ $CD3^+$
Macrophages	$CD68^+$

* Phenotyped by intensity thresholds in R programming software.

2.4 Statistical analyses

Immune cell mean density values and density quartiles were calculated with R separately in the CT and IM for all phenotyped cell categories. Mean values were calculated and used in analyses for patients from whom more than one CT or IM core was used. Cell densities were calculated as cells/mm^2. Cell density data together with patient data was used to create Kaplan-Meier survival curves in IBM SPSS Statistics software (version 27) to determine cancer-specific survival rates three and five years after operation. Receiver operating characteristics (ROC) analysis was used to optimal cut-offs using five-year cancer-specific survival after primary tumor resection as a state variable. The used ROC-cutoffs are presented in Appendix 4. An overview of patient demographics of the research sample material with data factors considered important in cancer survival are presented in Table 3.

TABLE 3: Demographic table of patient factors that may affect survival when investigating long-term survival in lung cancer patients.

Factor	Number (%)
Sex	
Male	127 (64,8%)
Female	69 (35,2%)
Age (median)	71,5
Smoker*	
Yes	156 (82,5%)
No	33 (17,5%)
TNM stage	
0-II	122 (62,2%)
III	48 (24,5%)
IV	26 (13,3%)
Fitness	
Skill level	
1	14 (7,7%)
2	115 (62,8%)
3	49 (26,8%)
4	5 (2,7%)
Stair climb	
<10 m	16 (8,2%)
10–14 m	28 (14,4%)
>14 m	151 (77,4%)
Neoadjuvant treatments	
Yes	21 (10,7%)
No	175 (89,3%)

* "Yes" includes current and ex-smokers. "No" includes never-smokers.

2.5 Licenses

The project is part of larger study conducted in cooperation between two healthcare districts. The study was approved by the Oulu University Ethics Committee (EETTMK 81/2008). The National Authority for Medicolegal Affairs (VALVIRA) waived the need for informed consent and approved for the use of data and samples. The usage of the patient sample material in the research is covered by licenses THL/143/5.05.00/2015 and THL/1349/5.05.00/2015. All persons involved in the thesis, and persons interested in further research from the thesis material, have been added to the licenses.

All material and data have been handled with complete pseudonymity. Personal and patient information has only been handled by medical professionals with access to the databases of Hospital Nova of Central Finland. Individual samples cannot be connected to the patient in the final thesis.

3 RESULTS

At least three 1.5 mm diameter core samples were taken from 198 NSCLC donor tumor blocks, of which nine TMA blocks were made. Cores from two samples were damaged during the sectioning and staining process, which led to 196 samples in total for analyses.

Representative TMA blocks were successfully created. Accurately punched core samples from donor blocks made possible the detailed investigation of the immune cell composition in both the CT and IM (Figure 4). For quality control the intensity of each marker was measured in each TMA block to detect possible defects in the staining process (Appendix 5). As the marker intensity stays consistent with no large fluctuations between TMA blocks, it could be ensured that all the samples have been treated and stained the same way for reliable results.

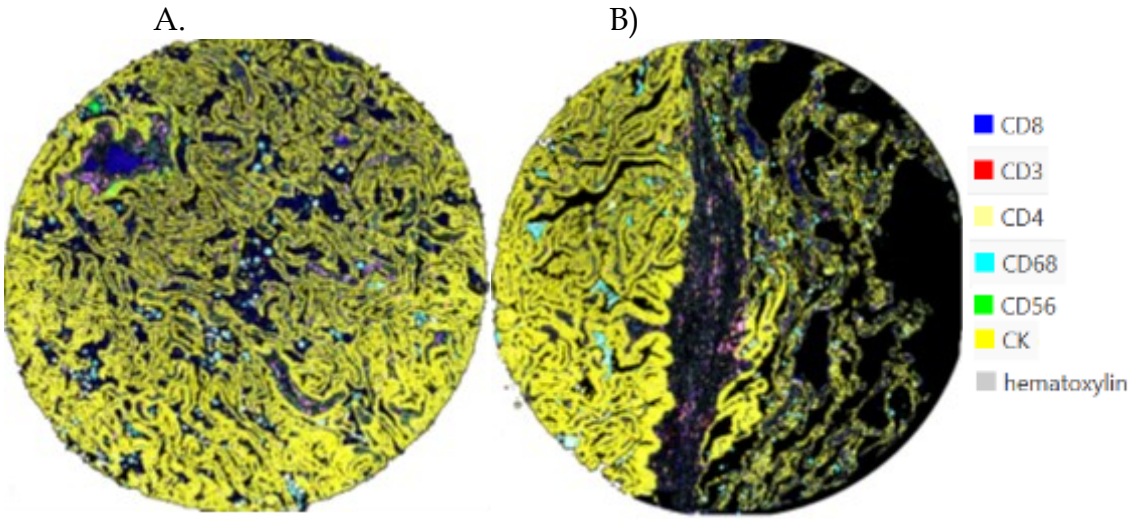

Figure 4: Core samples of a lung tumor stained with several markers using the multiplex panel. A) A core sample taken from the central tumor material. B) A core taken from the IM. Tumor material is seen on the left, the tumor edge runs through the middle, and normal lung tissue is seen on the right side. Seven marker channels are visible in the images.

Multiplex staining proved successful in providing a comprehensive overview of immune cell composition in lung tumors (Figure 5). Different groups if immune cells could be examined separately by selecting markers specific to them.

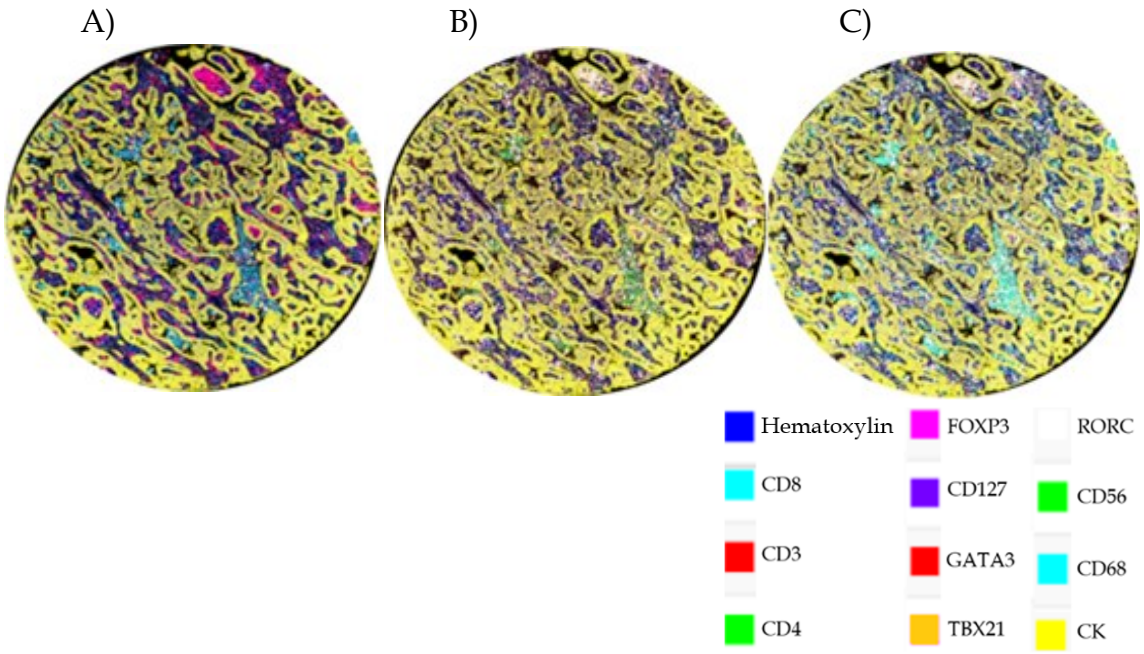

Figure 5: Lung tumor core samples stained with a panel of 12 immune cell markers. A) A panel of all ILCs ($CD127^+$), all T lymphocytes ($CD3^+$), NK cells ($CD56^+$) and macrophages ($CD68^+$). B) A T lymphocyte panel to show cytotoxic T lymphocytes ($CD3^+$ $CD8^+$) T helper lymphocytes ($CD3^+$ $CD4^+$), regulatory T lymphocytes ($CD3^+$ $CD4^+$ $FOXP3^+$), and T helper subtypes Th_1 ($CD3^+$ $CD4^+$ $TBX21^+$), Th_2 ($CD3^+$ $CD4^+$ $GATA3^+$) and Th_{17} ($CD3^+$ $CD4^+$ $RORC^+$). C) All markers are visible. In all images hematoxylin and cytokeratin (CK) are visible to indicate cell nuclei and tumor cells, respectively.

Cell amounts were calculated in R. A total of 11 342 818 cells were detected in the sample material. Out of these over eight percent were cytotoxic T lymphocytes, just under two percent were macrophages and almost ten percent were T helper lymphocytes as seen in Table 4. Out of T helper cells 64,43% were categorized as one of the four subtypes. Most of the subtypes were Th_2 cells (35,09%) and the least were Th_1 cells (5,88%).

TABLE 4: Total cell type amounts and percentages of cytotoxic T lymphocytes, T helper lymphocytes and macrophages (A), and T helper subtypes (B) from all sample cores.

A)

Cell type	Number of cells	Percentage
Total	11 342 818	100%
Cytotoxic T lymphocyte	943 835	8,32%
T helper lymphocyte	1 121 560	9,89%
Macrophage	220 933	1,95%

B)

Cell type	Number of cells	Percentage of T helper lymphocytes
T helper lymphocytes	1 121 560	100%
Regulatory T lymphocytes	169 024	15,07%
Th_1	65 915	5,88%
Th_2	393 539	35,09%
Th_{17}	94 109	8,39%
Total subtype amount of T helper lymphocytes	722 587	64,43%

The amounts of cells were calculated for helper, regulatory, and cytotoxic T lymphocytes in the CT and IM sample cores. Cell numbers were compared to investigate differences between cell compositions in the CT and IM. No significant difference was found in T helper lymphocytes and regulatory T lymphocytes with p values of 0.21 and 0.7, respectively. However, as seen in Figure 6, there are more cytotoxic T lymphocytes found in the IM than in the CT ($p = 0.0011$).

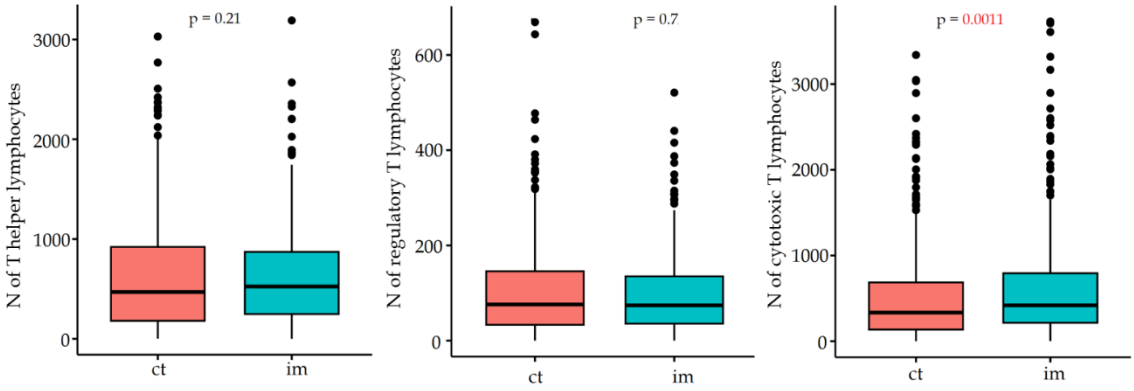

Figure 6: Number of cells calculated for T helper lymphocytes, regulatory T lymphocytes and cytotoxic T lymphocytes in the tumor center (ct) and invasive

margin (im). Helper and regulatory lymphocytes display no significant difference in tumor area distribution with p values of 0.21 and 0.7, respectively. Cytotoxic T lymphocytes, however, appear in larger numbers in the IM than in the CT as shown by the p value of 0.0011.

Cancer-specific survival three and five years after operation was calculated for Th_1, Th_2 and Th_{17} lymphocytes. Calculations were made separately for the CT and IM. Kaplan-Meier curves show cancer-specific survival three years after operation (Figure 7). Th_{17} lymphocytes have a statistical significance on survival when found in high concentrations in the CT (p=0.014).

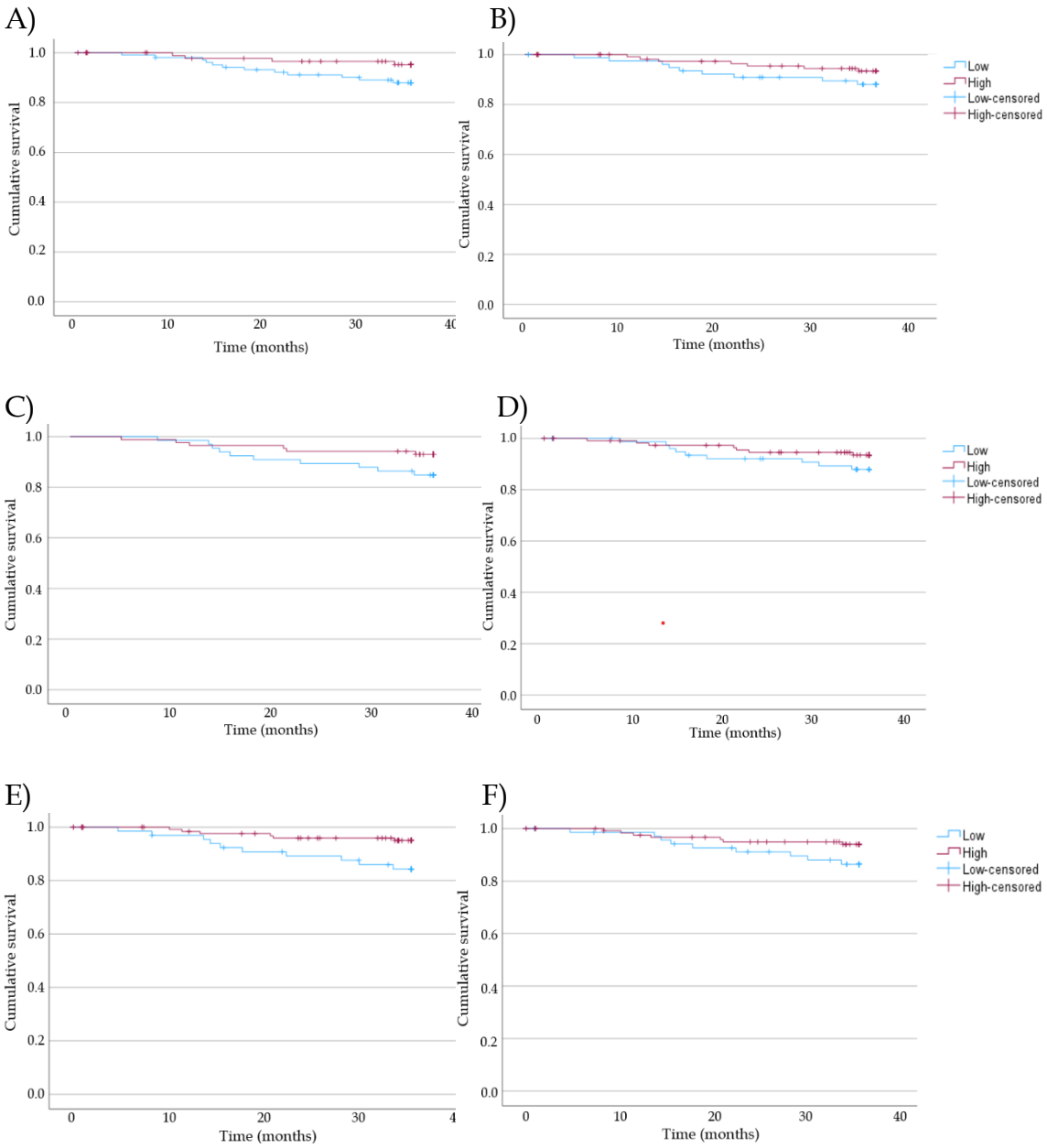

Figure 7: Kaplan-Meier cancer-specific survival curves three years after operation stratified for overall Th_1, Th_2, and Th_{17} lymphocytes using ROC cutoff. The

graphs show the difference in cumulative survival between high Th_1 (A and B), Th_2 (C and D), and Th_{17} (E and F) concentration (red) and low concentration (blue). A) Th_1 concentration in the CT has no impact on survival (p=0.082). B) Th_1 concentration in the IM has no impact on survival (p=0.199). C) Th_2 concentration in the CT has no impact on survival (p=0.158). D) Th_2 concentration in the IM has no impact on survival (p=0.196). E) High Th_{17} in the CT has a statistically significant impact on better cancer-specific survival three years after operation (p=0.014). F) Th_{17} concentration in the IM has no impact on survival (p=0.091).

Th_{17} lymphocytes have a statistical significance on long-term survival in lung cancer both in the CT (p= 0.002) and in the IM (p=0.017) five years after operation (Figure 8). Th_1 and Th_2 lymphocytes do not have a statistically significant impact on cancer-specific survival in lung cancer five years post operation (not shown).

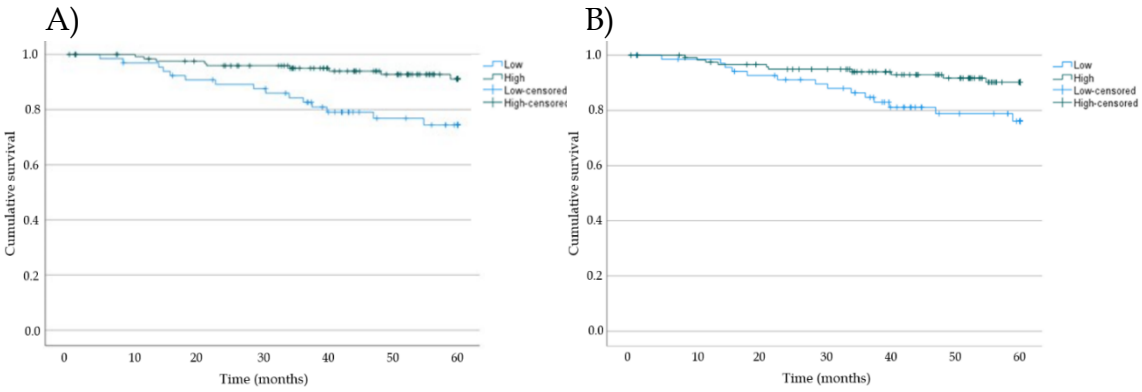

Figure 8: Kaplan-Meier cancer-specific survival curves for five years after operation for Th_{17} concentrations in the CT and IM. The graphs show the difference in cumulative survival between high Th_{17} concentration (green) and low Th_{17} concentration (blue). A) High Th_{17} concentration in the CT has a statistically significant impact on better cancer-specific survival (p=0.002). B) High Th_{17} concentration in the IM has a statistically significant impact on better cancer-specific survival (p=0.017).

4 DISCUSSION

One of the primary aims of the study was to research ILCs in lung cancer. Among immune cell research T lymphocytes have held a position as the most interesting and significant in cancer studies, which is why it was an intriguing idea to investigate the role of ILCs in cancer survival, how prevalent different ILC types are in lung tumors and what differences can be found between different cases. Unfortunately, after several concentration tests and trials, the CD127 marker failed to work sufficiently, and the data acquired is not reliable. A specific marker for ILC cells would be needed for ILC research to become easier and more

reliable. Due to the failure of investigating ILCs it was decided to focus on T helper subtypes Th_1, Th_2, and Th_{17}, as they are comparable by function to ILC1, ILC2, and ILC3, respectively, and have not been extensively studied in lung cancer.

The sample material came down from 244 to 196 samples. There are several reasons for this reduction. Some sample blocks were not found from the archives and others proved to be unsuitable for research purposes as the tumor was too small, it may have become too necrotic or there may not have been any cancerous material left at all. The downside to using TMA blocks is that sample cores are under much stress during a long multiplex staining process, which also caused two samples to be lost as cores were torn, broken, or detached. Still the objective of creating representative TMA blocks and a comprehensive multiplex immunopanel for lung cancer tumor immune microenvironment research could be achieved (Figure 4, Figure 5), and with 196 analyzed samples statistically significant results were acquired.

The clinical significance of high amounts of cytotoxic $CD8^+$ T lymphocytes in better cancer outcome has been well established. Cytotoxic T lymphocytes were shown in Figure 6 to appear in larger amounts in the IM compared to the CT. This is in line with previous research. In colorectal cancer, Elomaa et al. (2022) found higher amounts of $CD8^+$ T lymphocytes in the IM compared to the CT. Similar results were found in breast cancer studies (Miyan et al. 2016, Fortis et al. 2017). Spatial distribution research of $CD8^+$ T lymphocytes has not been done extensively in lung cancer, except in relation to regulatory T lymphocytes (Barua et al. 2018) and PD-1 (Bocchialini et al. 2020). Barua et al. and Bocchialini et al. found that a high concentration of $CD8^+$ lymphocytes impact long term survival, with a high abundance of $CD8^+$ lymphocytes among regulatory T lymphocytes even mitigating the negative effects they have on cancer development. Donnem et al. (2015) found that $CD8^+$ T lymphocytes in the IM had the most impact on a better prognosis in lung cancer.

The hypothesis of ILC1 cells having an impact on long-term survival in lung cancer could not be accepted as the marker CD127 failed to work sufficiently. However, the comparable Th_1 did not show significance in cancer-specific survival three and five years after operation. This is interesting as Th_1 functions in anti-tumor, as well as antiviral and antibacterial, activities that may be helpful in post-operation recovery. On the other hand, Th_{17} cells did show a statistical significance on cancer-specific survival in the CT three years and in the CT and IM five years after operation (Figure 7 and Figure 8, respectively). Interestingly, Th_{17} cells are the second least prevalent of the helper T lymphocyte subcategories but still the one to show a correlation with survival (Table 4).

It has been found that Th_{17} has the plasticity to take on a Th_1 or regulatory T lymphocyte phenotype and therefore express anti-tumor or protumor activity, respectively. Previous research shows contradicting and protumor results related to Th_{17} in lung cancer. The type of cancer impacts the ways in which Th_{17} cells react and contribute to cancer development, and the complex signaling pathways between Th_{17}, immune cells, and tumor cells are not fully understood. In their

review article Duan et al. (2014) discuss the role of Th_1/Th_2 balance in lung cancer development and bring up research that suggests they have an impact on cancer onset and progression, as well as noting the possible protection of T-BET expressing Th_1 cells against lung tumor growth, which is in line with the hypothesis of the thesis study. They also bring up the close relationship and balance of regulatory T lymphocytes and Th_{17} cells as an important factor in lung cancer progression. It seems the cytokines produced, their balance and the ratio of Th_{17} to regulatory T lymphocytes comprise a network that is significant in understanding lung cancer development. TGF-β, a regulator of Th_{17} differentiation, has both anti-tumor and protumor activity depending on the stage of the disease. Similarly, IL-17a, produced by Th_{17}, can elicit both properties (Marques et al. 2021). Zhou et al. (2008) have found that in the blood of NSCLC patients there is a significant increase in regulatory T lymphocytes and FOXP3 expression and a decrease in Th_{17} cells, RORC and IL-17 expression while compared to that in healthy patients, and the Th_{17}/regulatory T lymphocyte ratio is negatively correlated with the TNM stages. In early stage lung cancer differentiation into Th_{17} may be promoted, while in later stages the overproduction of regulatory T lymphocyte cytokines promotes a change in the Th_{17}/regulatory T lymphocyte balance toward a protumor response by regulatory T lymphocytes and inhibits the Th_{17} response. The complex relationships between cytokines produced and their effect on the T helper subtypes and lung cancer progression are not fully understood but may hold remarkable clinical significance.

Wang et al. 2018 studied how IL-17a from Th_{17} cells affects NSCLC tumor growth. As Zhou et al. previously, Wang et al. also found elevated levels of Th_{17} cells and IL-17a in peripheral blood of NSCLC patients compared to healthy blood donors. They also concluded that high Th_{17} density correlated with a poorer prognosis in NSCLC. Salazar et al. (2020) conducted experiments on mice and human lung tissue. Their findings show that Th_{17} (and Th_9) in lung cancer promote tumor progression and metastasis. When examining the effect of Th_{17} with immunological treatments, such as PD-L1 inhibitors, it has been shown that IL-17 creates resistance in tumor cells against PD-L1 inhibitors whilst also contributing to tumor invasion and metastasis (Peng et al. 2021). Although research has shown that Th_{17} may exhibit anti-tumor properties, results predominantly show tumor promoting evidence when investigated alone, by their secreted cytokines, or in correlation with other immune cells. The result of better survival with high Th_{17} concentration in the thesis research go against these findings in literature, but the relationship between Th_{17} and lung cancer is comprised of complex communication, which is yet to be fully understood. More research on this topic is needed to reveal potential clinical therapeutical targets.

There are some limitations in the thesis project. Whilst a broad selection of immune cell markers was selected for the multiplex panel, only T helper subtypes were investigated in correlation with cancer-specific survival after operation. Therefore, the results of Th_{17} having a positive impact on survival are detached from the consensus of Th_{17} cells having a mostly negative impact on cancer

progression and tumor metastasis found in previous research as no other factors were taken into consideration. From a methodological point of view, the license process for the thesis was prolonged. As patient data was used and analyzed, appropriate licenses needed to be applied and approved, and work could not start until all licenses were in order. During the license application period many delays were encountered as the complex bureaucracy had to be solved. This is something to consider when taking on a project handling patient data from different healthcare districts. The methods used in the project, albeit convenient and time sparing as well as cost-effective, are not suitable for clinical use. Multiplex immunohistochemistry and TMA blocks are effective tools for research, and even though there is evidence to support the reliability and representability of TMA blocks, clinical diagnostics still rely on whole biopsy samples and traditional immunohistochemistry for maximal reliability. Perhaps in the future these methods will become more established and get used in diagnostics.

5 CONCLUSION

Th_{17} seems to be quite the paradoxical factor in cancer, as secreted interleukins and interactions with other immune cells, and the tumor itself, affect its influence on tumor growth and cancer progression, hence both protumor and anti-tumor effects are possible. The relationship between Th_{17} and NSCLC needs to be investigated further in relation to other factors, as the positive impact on long-term survival found in this research lacks the answer as to why this result was achieved. There seems to be a great possibility Th_{17} may be a target for immunotherapy in the future.

ACKNOWLEDGEMENTS

I would like to thank my supervisors Ph. D. Jari Ylänne and D. Sc. Jatta Saarenheimo for support and guidance during the thesis process, and M. Sc. Hanna Elomaa for hands-on tutelage in the laboratory. I would also like to thank Ph. D. Maarit Ahtiainen, MD Olli Helminen and MD Eero Sihvo for patient data expertise, and research director, MD Teijo Kuopio, MD Juha Väyrynen and MD Jukka-Pekka Mecklin for irreplaceable consulting. The thesis project will be part of more research done on the material in future projects.

Jyväskylä 23.11.2023
Essi Kivelä

REFERENCES

Albini, A., Magnani, E., & Noonan, D. M. 2010. The tumor microenvironment: biology of a complex cellular and tissue society. *Q J Nucl Med Mol Imaging* 54: 244-8.

Alsaab, H. O., Sau, S., Alzhrani, R., Tatiparti, K., Bhise, K., Kashaw, S. K., & Iyer, A. K. 2017. PD-1 and PD-L1 Checkpoint Signaling Inhibition for Cancer Immunotherapy: Mechanism, Combinations, and Clinical Outcome. *Front Pharmacol*. 23;8:561. doi: 10.3389/fphar.2017.00561. PMID: 28878676.

Anderson, N. M., & Simon, M. C. 2020. The tumor microenvironment. *Current Biology* 30: 921–925.

Anderson, N. R., Minutolo, N. G., Gill, S., & Klichinsky, M. 2021. Macrophage-Based Approaches for Cancer Immunotherapy. *Cancer Research* 81: 1201–1208.

Annunziato, F., Romagnani, C., & Romagnani, S. 2015. The 3 major types of innate and adaptive cell-mediated effector immunity. *The Journal of Allergy and Clinical Immunology* 135: 626–635.

Barua, S., Fang, P., Sharma, A., Fujimoto, J., Wistuba, I., Rao, A. U. K., & Lin, S. H. 2018. Spatial interaction of tumor cells and regulatory T cells correlates with survival in non-small cell lung cancer. *Lung Cancer* (Amsterdam, Netherlands) 117: 73–79.

Bocchialini, G., Lagrasta, C., Madeddu, D., Mazzaschi, G., Marturano, D., Sogni, F., Silini, E. M., Gnetti, L., Becchi, G., Rusca, M., Carbognani, P., Ventura, L., Braggio, C., Tiseo, M., Quaini, F., & Ampollini, L. 2020. Spatial architecture of tumour-infiltrating lymphocytes as a prognostic parameter in resected non-small-cell lung cancer. *European Journal of Cardio-thoracic Surgery : Official Journal of the European Association for Cardio-thoracic Surgery* 58(3), 619–628.

Bowden D. H. 1984. The alveolar macrophage. *Environmental Health Perspectives* 55: 327–341.

Browning, J. L., Miatkowski, K., Sizing, I., Griffiths, D., Zafari, M., Benjamin, C. D., Meier, W., & Mackay, F. 1996. Signaling through the lymphotoxin beta receptor induces the death of some adenocarcinoma tumor lines. *The Journal of Experimental Medicine* 183: 867–878.

Bubendorf, L., Nocito, A., Moch, H., & Sauter, G. 2001. Tissue microarray (TMA) technology: miniaturized pathology archives for high-throughput in situ studies. *J Pathol*. 195(1): 72-9.

Cano, R. L. E. & Lopera, H. D. E. 2013. Introduction to T and B lymphocytes. In: Anaya, J. M., Shoenfeld, Y., Rojas-Villarraga A, et al. *Autoimmunity: From Bench to Bedside.* Bogota (Colombia): El Rosario University Press; Chapter 5. Available from: https://www.ncbi.nlm.nih.gov/books/NBK459471/

Cha, J. H., Chan, L. C., Li, C. W., Hsu, J. L., & Hung, M. C. 2019. Mechanisms Controlling PD-L1 Expression in Cancer. *Mol Cell* 76: 359-370.

Chang S. H. (2019). T helper 17 (Th17) cells and interleukin-17 (IL-17) in cancer. *Archives of Pharmacal Research*, 42(7), 549–559.

Chauhan, A. F. & Liu, S. V. 2020. Small Cell Lung Cancer: Advances in Diagnosis and Management. *Semin Respir Crit Care Med* 41: 435-446.

Chen, D. S. & Mellman, I. 2013. Oncology meets immunology: The cancer-immunity cycle. *Science Direct* 39: 1-10.

de Boer, O. J., Krebbers, G., Mackaaij, C., Florquin, S., de Rie, M. A., van der Wal, A. C., & Teunissen, M. 2020. Comparison of Two Different Immunohistochemical Quadruple Staining Approaches to Identify Innate Lymphoid Cells in Formalin-fixed Paraffin-embedded Human Tissue. *The Journal of Histochemistry and Cytochemistry : Official Journal of the Histochemistry Society* 68: 127–138.

De Grove, K. C., Provoost, S., Verhamme, F. M., Bracke, K. R., Joos, G. F., Maes, T., & Brusselle, G. G. 2016. Characterization and Quantification of Innate Lymphoid Cell Subsets in Human Lung. *PloS One*, 11(1), e0145961. https://doi.org/10.1371/journal.pone.0145961

Detterbeck, F. C., Boffa, D. J., Kim, A. W., & Tanoue, L. T. 2017. The Eighth Edition Lung Cancer Stage Classification. *Chest* 151: 193–203.

Diaz-Moralli, S., Tarrado-Castellarnau, M., Miranda, A., & Cascante, M. 2013. Targeting cell cycle regulation in cancer therapy. *Pharmacology & Therapeutics*, 138(2), 255-271. ISSN 0163-7258.

Donnem, T., Hald, S. M., Paulsen, E. E., Richardsen, E., Al-Saad, S., Kilvaer, T. K., Brustugun, O. T., Helland, A., Lund-Iversen, M., Poehl, M., Olsen, K. E., Ditzel, H. J., Hansen, O., Al-Shibli, K., Kiselev, Y., Sandanger, T. M., Andersen, S., Pezzella, F., Bremnes, R. M., & Busund, L. T. 2015. Stromal CD8+ T-cell Density—A Promising Supplement to TNM Staging in Non-Small Cell Lung Cancer. *Clinical Cancer Research : An Official Journal of the American Association for Cancer Research* 21(11): 2635–2643.

Duan, M. C., Zhong, X. N., Liu, G. N., & Wei, J. R. 2014. The Treg/Th17 paradigm in lung cancer. *J Immunol Res, 2014*, 730380. https://doi.org/10.1155/2014/730380

Eberl, G., Colonna, M., Di Santo, J. P., & McKenzie, A. N. 2015. Innate lymphoid cells. Innate lymphoid cells: a new paradigm in immunology. *Science (New York, N.Y.),* 348(6237), aaa6566. https://doi.org/10.1126/science.aaa6566

Elomaa, H., Ahtiainen, M., Väyrynen, S.A., Ogino, S., Nowak, J. A., Friman, M., Helminen, O., Wirta, E-V., Seppälä, T. T., Böhm, J., Mäkinen, M. J., Mecklin, J-P., Kuopio, T. & Väyrynen, J. P. 2022. Prognostic significance of spatial and density analysis of T lymphocytes in colorectal cancer. *Br J Cancer* 127: 514–523.

Eskaros, A. R., Egloff, S. A., Boyd, K. L., Richardson, J. E., Hyndman, M. E., & Zijlstra, A. 2017. Larger core size has superior technical and analytical accuracy in bladder tissue microarray. *Laboratory Investigation; A Journal of Technical Methods and Pathology* 97: 335–342.

Fortis, S. P., Sofopoulos, M., Sotiriadou, N. N., Haritos, C., Vaxevanis, C. K., Anastasapoulou, E. A., Janssen, N., Arnogiannaki, N., Ardavanis, A., Pawelec, G., Perez, S. A. & Baxevanis, C. N. 2017. Differential intratumoral distributions of CD8 and CD163 immune cells as prognostic biomarkers in

breast cancer. *Journal for ImmunoTherapy of Cancer* 5: 39. doi: 10.1186/s40425-017-0240-7

Fridman, W. H., Galon, J., Pagès, F., Tartour, E., Sautès-Fridman, C. & Kroemer, G. 2011. Prognostic and Predictive Impact of Intra- and Peritumoral Immune Infiltrates. *Cancer Res* 71: 17.

Fridman, W. H., Pagès, F., Sautès-Fridman, C., & Galon J. 2012. The immune contexture in human tumours: impact on clinical outcome. *Nat Rev Cancer* 15;12(4): 298-306.

GLOBOCAN 2022. Cancer today. https://gco.iarc.fr/today/ (accessed 12.10.2022)

Gou, Q., Dong, C., Xu., H., Khan, B., Jin, J., Liu, Q., Shi, J. & Hou, Y. 2020. PD-L1 degradation pathway and immunotherapy for cancer. *Cell Death Dis*. 11; 955.

Gray, J.I., Westerhof, L.M. & MacLeod, M.K.L. 2018, The roles of resident, central and effector memory CD4 T-cells in protective immunity following infection or vaccination. *Immunology* 154: 574-581.

Hanahan, D. & Weinberg, R. A. 2011. Hallmarks of cancer: the next generation. *Cell* 4;144(5): 646-74.

Harrington, L. E., Hatton, R. D., Mangan, P. R., Turner, H., Murphy, T. L., Murphy, K. M., & Weaver, C. T. 2005. Interleukin 17-producing CD4+ effector T cells develop via a lineage distinct from the T helper type 1 and 2 lineages. *Nature Immunology* 6: 1123–1132.

Herbst, R., Morgensztern, D. & Boshoff, C. 2018. The biology and management of non-small cell lung cancer. *Nature* 553: 446–454.

Hofman, P., Badoual, C., Henderson, F., Berland, L., Hamila, M., Long-Mira, E., Lassalle, S., Roussel, H., Hofman, V., Tartour, E., & Ilié, M. 2019. Multiplexed Immunohistochemistry for Molecular and Immune Profiling in Lung Cancer-Just About Ready for Prime-Time?. *Cancers*, 11(3), 283.

Hu, C., Zhao, L., Liu, W., Fan, S., Liu, J., Liu, Y., Liu, X., Shu, L., Liu, X., Liu, P., Deng, C., Qiu, Z., Chen, C., Jiang, Y., Liang, Q., Yang, L., Shao, Y., He, Q., Yu, D., Zeng, Y., Li, Y., Pan, Y., Zhang, S., Shi, S., Peng, Y., & Wu, F. 2021. Genomic profiles and their associations with TMB, PD-L1 expression, and immune cell infiltration landscapes in synchronous multiple primary lung cancers. *Journal for Immunotherapy of Cancer*, 9(12), e003773.

Italiani, P., & Boraschi, D. 2014. From Monocytes to M1/M2 Macrophages: Phenotypical vs. Functional Differentiation. *Frontiers in Immunology*, 5, 514. https://doi.org/10.3389/fimmu.2014.00514

Jain, P., Jain, C., & Velcheti, V. 2018. Role of immune-checkpoint inhibitors in lung cancer. *Therapeutic Advances in Respiratory Disease*, *12*, 1753465817750075. https://doi.org/10.1177/1753465817750075

Kalinski, P. & Basse, P. 2019. Chapter 1 - Immune Checkpoint Inhibitors: Mechanisms and Emerging Therapeutic Opportunities. In: Ito, F. & Ernstoff, M. S. Immune Checkpoint Inhibitors in Cancer, Elsevier, 1-17, ISBN 9780323549486, https://doi.org/10.1016/B978-0-323-54948-6.00001-9.

Kallioniemi, O-P., Wagner, U., Kononen, J., & Sauter, G. 2001. Tissue microarray technology for high-throughput molecular profiling of cancer. *Human Molecular Genetics*, 10: 657–662.

Khuder, S. A., Dayal, H. H., Mutgi, A. B., Willey, J. C., & Dayal, G. 1998. Effect of cigarette smoking on major histological types of lung cancer in men. *Lung Cancer* 22: 15–21.

Klose, C. S. N., Flach, M., Möhle, L., Rogell, L., Hoyler, T., Ebert, K., Fabiunke, C., Pfeifer, D., Sexl, V., Fonseca-Pereira, D., Domingues, R. G., Veiga-Fernandes, H., Arnold, S. J., Busslinger, M., Dunay, I. R., Tanriver, Y., & Diefenbach, A. 2014. Differentiation of type 1 ILCs from a common progenitor to all helper-like innate lymphoid cell lineages. *Cell* 157: 340–356.

Kononen, J., Bubendorf, L., Kallioniemi, A., Bärlund, M., Schraml, P., Leighton, S., Torhorst, J., Mihatsch, M. J., Sauter, G., & Kallioniemi, O. P. 1998. Tissue microarrays for high-throughput molecular profiling of tumor specimens. *Nature Medicine* 4: 844–847.

Lappi-Blanco Sequeiros, E., Mäkinen, J., Kosma, V-M., & Pääkkö, P. 2021. Patologia. *Duodecim*.

Leong, A. S., & Wright, J. 1987. The contribution of immunohistochemical staining in tumour diagnosis. *Histopathology 11*: 1295–1305.

Liu, H. I., Chiang, C. J., Su, S. Y. Jhuang, J. R., Tsai, D. R., Yang, Y. W., Lin, L. J., Wang, Y. C., & Lee, W. C. 2023. Incidence trends and spatial distributions of lung adenocarcinoma and squamous cell carcinoma in Taiwan. *Sci Rep* 13: 1655.

Marques, H. S., de Brito, B. B., da Silva, F. A. F., Santos, M. L. C., de Souza, J. C. B., Correia, T. M. L., Lopes, L. W., Neres, N. S. M., Dórea, R. S. D. M., Dantas, A. C. S., Morbeck, L. L. B., Lima, I. S., de Almeida, A. A., Dias, M. R. J., & de Melo, F. F. 2021. Relationship between Th17 immune response and cancer. *World J Clin Oncol* 12(10): 845–867.

McFarland, A. P., Yalin, A., Wang, S. Y., Cortez, V. S., Landsberger, T., Sudan, R., Peng, V., Miller, H. L., Ricci, B., David, E., Faccio, R., Amit, I., & Colonna, M. 2021. Multi-tissue single-cell analysis deconstructs the complex programs of mouse natural killer and type 1 innate lymphoid cells in tissues and circulation. *Immunity* 54: 1320–1337.

Meza, R., Meernik, C., Jeon, J., & Cote, M. L. 2015. Lung cancer incidence trends by gender, race and histology in the United States, 1973-2010. *PloS One* 10(3). https://doi.org/10.1371/journal.pone.0121323

Miyan, M., Schmidt-Mende, J., Kiessling, R., Poschke, I. & de Boniface, J. 2016. Differential tumor infiltration by T-cells characterizes intrinsic molecular subtypes in breast cancer. *J Transl Med* 14, 227. https://doi.org/10.1186/s12967-016-0983-9

Mosmann, T. R., Cherwinski, H., Bond, M. W., Giedlin, M. A. & Coffman, R. L. 1986. Two types of murine helper T cell clone. I. Definition according to profiles of lymphokine activities and secreted proteins. *J Immunol* 136: 2348-2357.

Nedergaard, B. S., Ladekarl, M., Thomsen, H. F., Nyengaard, J. R., & Nielsen, K. 2007. Low density of CD3+, CD4+ and CD8+ cells is associated with increased risk of relapse in squamous cell cervical cancer. *British Journal of Cancer*, 97: 1135–1138.

Nocito, A., Bubendorf, L., Tinner, E. M., Süess, K., Wagner, U., Forster, T., Kononen, J., Fijan, A., Bruderer, J., Schmid, U., Ackermann, D., Maurer, R., Alund, G., Knönagel, H., Rist, M., Anabitarte, M., Hering, F., Hardmeier, T., Schoenenberger, A. J., Flury, R., Jäger, P., Fehr, J. L., Schraml, P., Moch, H., Mihatsch, M. J., Gasser, T. & Sauter, G. 2001. Microarrays of bladder cancer tissue are highly representative of proliferation index and histological grade. *The Journal of Pathology* 194: 349–357.

Nooreldeen, R. & Bach H. 2021. Current and Future Development in Lung Cancer Diagnosis. *International Journal of Molecular Sciences*. 22(16):8661. https://doi.org/10.3390/ijms22168661

Oncohema Key. 2023. Introduction to Histology. Tissue Microarray Construction and Evaluation. https://oncohemakey.com/introduction-to-histology/ Visited 1.11.2023.

Peng, D. H., Rodriguez, B. L., Diao, L., Gaudreau, P. O., Padhye, A., Konen, J. M., Ochieng, J. K., Class, C. A., Fradette, J. J., Gibson, L., Chen, L., Wang, J., Byers, L. A., & Gibbons, D. L. 2021. Th17 cells contribute to combination MEK inhibitor and anti-PD-L1 therapy resistance in KRAS/p53 mutant lung cancers. *Nature Communications* 12(1): 2606. https://doi.org/10.1038/s41467-021-22875-w

Ramos-Vara, J. A. 2017. Principles and Methods of Immunohistochemistry. *Methods in Molecular Biology (Clifton, N.J.)* 1641: 115–128.

Riihimäki, M., Hemminki, A., Fallah, M., Thomsen, H., Sundquist, K., Sundquist, J., & Hemminki, K. 2014. Metastatic sites and survival in lung cancer. *Lung Cancer* 86: 78-84.

Rivera, G. A., & Wakelee, H. 2016. Lung Cancer in Never Smokers. *Advances in Experimental Medicine and Biology* 893: 43–57.

Romagnani, S. 1994. Lymphokine production by human T cells in disease states. *Annual Review of Immunology* 12: 227–257.

Salazar, Y., Zheng, X., Brunn, D., Raifer, H., Picard, F., Zhang, Y., Winter, H., Guenther, S., Weigert, A., Weigmann, B., Dumoutier, L., Renauld, J. C., Waisman, A., Schmall, A., Tufman, A., Fink, L., Brüne, B., Bopp, T., Grimminger, F., Seeger, W., Pullamsetti., S. S., Huber, M., & Savai, R. 2020. Microenvironmental Th9 and Th17 lymphocytes induce metastatic spreading in lung cancer. *The Journal of Clinical Investigation*, 130(7): 3560–3575.

Schraml, P., Kononen, J., Bubendorf, L., Moch, H., Bissig, H., Nocito, A., Mihatsch, M. J., Kallioniemi, O. P., & Sauter, G. 1999. Tissue microarrays for gene amplification surveys in many different tumor types. *Clinical Cancer Research : An Official Journal of the American Association for Cancer Research* 5: 1966–1975.

Schroder, K., Hertzog, P. J., Ravasi, T., & Hume, D. A. 2004. Interferon-gamma: an overview of signals, mechanisms and functions. *Journal of Leukocyte Biology* 75: 163–189.

Sharma, P., Siddiqui, B. A., Anandhan, S., Yadav, S. S., Subudhi, S. K., Gao, J., Goswami, S., & Allison, J. P. 2021. The Next Decade of Immune Checkpoint Therapy. *Cancer Discovery* 11: 838–857.

Sounni, N. E., & Noel, A. 2013. Targeting the tumor microenvironment for cancer therapy. *Clinical Chemistry* 59: 85–93.

Spits, H., & Cupedo, T. 2012. Innate lymphoid cells: emerging insights in development, lineage relationships, and function. *Annual Review of Immunology* 30: 647–675.

Stabile, H., Fionda, C., Gismondi, A., & Santoni, A. 2017. Role of Distinct Natural Killer Cell Subsets in Anticancer Response. *Front Immunol*. 8, 293. doi:10.3389/fimmu.2017.00293

Sung, H., Ferlay, J., Siegel, R. L., Laversanne, M., Soerjomataram, I., Jemal, A., & Bray, F. 2021. Global Cancer Statistics 2020: GLOBOCAN Estimates of Incidence and Mortality Worldwide for 36 Cancers in 185 Countries. *CA: a Cancer Journal for Clinicians* 71(3): 209–249.

Syn, N. L., Teng, M. W. L., Mok, T. S. K., & Soo, R. A. 2017. De-novo and acquired resistance to immune checkpoint targeting. *The Lancet. Oncology* 18: 731–741.

Tan, W., Nerurkar, S. N., Cai, H. Y., Ng, H., Wu, D., Wee, Y., Lim, J., Yeong, J., & Lim, T. 2020. Overview of multiplex immunohistochemistry/immunofluorescence techniques in the era of cancer immunotherapy. *Cancer Communications* 40: 135–153.

Triulzi, T., Tagliabue, E., Balsari, A., & Casalini, P. 2012. FOXP3 expression in tumor cells and implications for cancer progression. *Journal of Cellular Physiology* 228; 1. https://doi.org/10.1002/jcp.24125

Tsujikawa, T., Kumar, S., Borkar, R. N., Azimi, V., Thibault, G., Chang, Y. H., Balter, A., Kawashima, R., Choe, G., Sauer, D., El Rassi, E., Clayburgh, D. R., Kulesz-Martin, M. F., Lutz, E. R., Zheng, L., Jaffee, E. M., Leyshock, P., Margolin, A. A., Mori, M., Gray, J. W., Flint, P. W. & Coussens, L. M. 2017. Quantitative Multiplex Immunohistochemistry Reveals Myeloid-Inflamed Tumor-Immune Complexity Associated with Poor Prognosis. *Cell Reports* 19: 203–217.

van der Leun, A. M., Thommen, D. S., & Schumacher, T. N. 2020. CD8+ T Cell States in Human Cancer: Insights from Single-Cell Analysis. *Nat. Rev. Cancer* 20: 218–232.

Vivier, E., Artis, D., Colonna, M., Diefenbach, A., Di Santo, J. P., Eberl, G., Koyasu, S., Locksley, R. M., McKenzie, A. N. J., Mebius, R. E., Powrie, F., & Spits, H. 2018. Innate Lymphoid Cells: 10 Years On. *Cell* 174: 1054–1066.

Wang, R., Yang, L., Zhang, C., Wang, R., Zhang, Z., He, Q., Chen, X., Zhang, B., Qin, Z., Wang, L., & Zhang, Y. 2018. Th17 cell-derived IL-17A promoted tumor progression via STAT3/NF-κB/Notch1 signaling in non-small cell

lung cancer. *Oncoimmunology* 7(11), e1461303. https://doi.org/10.1080/2162402X.2018.1461303

Wang, M., Herbst, R. S., & Boshoff, C. 2021. Toward personalized treatment approaches for non-small-cell lung cancer. *Nat Med* 27: 1345-1356.

Wouters, M. C. A., & Nelson, B. H. 2018. Prognostic Significance of Tumor-Infiltrating B Cells and Plasma Cells in Human Cancer. *Clin. Cancer Res* 24: 6125–6135.

Yang, L., & Zhang, Y. 2017. Tumor-associated macrophages: from basic research to clinical application. *Journal of Hematology & Oncology* 10: 58.

Ye, J., Su, X., Hsueh, E. C., Zhang, Y., Koenig, J. M., Hoft, D. F., & Peng, G. (2011). Human tumor-infiltrating Th17 cells have the capacity to differentiate into IFN-γ+ and FOXP3+ T cells with potent suppressive function. *European Journal of Immunology*, 41(4), 936–951.

Zappa, C., & Mousa, S. A. 2016. Non-small cell lung cancer: current treatment and future advances. *Translational Lung Cancer Research* 5: 288–300.

Zeng, C., Yao, Y., Jie, W., Zhang, M., Hu, X., Zhao, Y., Wang, S., Yin, J., & Song, Y. 2013. Up regulation of Foxp3 participates in progression of cervical cancer. *Cancer Immunol Immunother* 62: 481-7.

Zheng, X., Weigert, A., Reu, S., Guenther, S., Mansouri, S., Bassaly, B., Gattenlöhner, S., Grimminger, F., Pullamsetti, S., Seeger, W., Winter, H., & Savai, R. 2020. Spatial Density and Distribution of Tumor-Associated Macrophages Predict Survival in Non-Small Cell Lung Carcinoma. *Cancer Research* 80: 4414–4425.

Zhou, J., Tian, Z., & Peng, H. 2020. Tissue-resident NK cells and other innate lymphoid cells. *Advances in Immunology* 145: 37–53.

APPENDIX 1. MULTIPLEX STAINING PROTOCOL

TABLE: Multiplex immunohistochemical staining protocol. A) Multiplex protocol for the first staining cycle. B) Multiplex protocol for the consecutive cycles.

A)

Bake and dewax	**Reagent**	**Time (min)**	**Temperature (C°)**
1	No reagent	30	60
2	Bond Dewax solution	0.5	72
3	Bond Dewax solution	0	72
4	Bond Dewax solution	0	RT
Antigen retrieval			
1	Bond ER solution 2	0	RT
2	Bond ER solution 2	0	RT
3	Bond ER solution 2	30	100
4	Bond ER solution 2	0	RT
Staining protocol with AEC			
1	Peroxidase block	5	
2	Bond wash solution	0	
3	Bond wash solution	0	
4	Bond wash solution	0	
5	Marker	30	
6	Bond wash solution	0	
7	Bond wash solution	0	
8	Bond wash solution	0	
9	Post-primary	8	
10	Bond wash solution	2	
11	Bond wash solution	2	
12	Polymer	8	
13	Bond wash solution	2	
14	Bond wash solution	2	
15	H_2O	0	
16	AEC	0	
17	AEC	20	
18	H_2O	0	
19	H_2O	0	
20	H_2O	0	
21	Hematoxylin	10	
22	H_2O	0	
23	Bond wash solution	0	
24	H_2O	0	

B)

Antigen retrieval	**Reagent**	**Time (min)**	**Temperature (Cº)**
1	Bond ER solution 1	0	RT
2	Bond ER solution 1	0	RT
3	Bond ER solution 1	20-60	100
4	Bond ER solution 1	0	RT
Staining protocol with AEC			
1	Ethanol	0	
2	Ethanol	0	
3	Ethanol	1	
4	Ethanol	0	
5	Ethanol	0	
6	Bond wash solution	0	
7	Bond wash solution	0	
8	Bond wash solution	0	
9	Bond wash solution	1	
10	Bond wash solution	0	
11	Bond wash solution	0	
12	Bond wash solution	0	
13	Marker	30	
14	Bond wash solution	0	
15	Bond wash solution	0	
16	Bond wash solution	0	
17	Post primary	8	
18	Bond wash solution	2	
19	Bond wash solution	2	
20	Polymer	0	
21	Bond wash solution	2	
22	Bond wash solution	2	
23	H_2O	0	
24	AEC	0	
25	AEC	20	
26	H_2O	0	
27	H_2O	0	
28	H_2O	0	
29	Hematoxylin	10	
30	H_2O	0	
31	Bond wash solution	0	
32	H_2O	0	

APPENDIX 2. MARKER DETAILS

TABLE: Details of markers used in multiplex staining.

Cycle	Marker	Clone	Manufacturer (Cat. #)	Host species	Antigen retrieval	Target
1	CD8	4B11	Leica (PA0183)	mouse	ER2, 30 min	Cytotoxic T cell
2	CD3	LN10	Leica (PA055)	mouse	ER1, 30 min	T cell
3	CD4	EP204	Cell Marque (104R-2)	rabbit	ER1, 30 min	Helper T cell
4	FOXP3	236A/E7	Abcam (ab20034)	mouse	ER1, 60 min	Reg. T cell
5	CD127	EPR23747-333	Abcam (ab259806)	rabbit	ER1, 60 min	ILC
6	T-BET	ab150440	Abcam (ab150440)	mouse	ER1, 60 min	ILC, Th_1
7	GATA3	L50-823	Cell Marque (390-M-15)	rabbit	ER1, 60 min	ILC, Th_2
8	RORC	6F3.1	Biocare Medical (ACI 3208)	mouse	ER1, 60 min	ILC, Th_{17}
9	CD56	MRQ-42	Cell Marque (156R-96)	rabbit	ER1, 30 min	NK/NKT
10	CD68	KP1	BioLegend (916104)	mouse	ER1, 60 min	Macrophage
11	CD163	10D6	Thermo Scientific (MS-1103)	mouse	ER1, 20 min	Macrophage
12	KRT	BS5	BioSite Histo (BSH-7124-1)	mouse	ER1, 60 min	Epithelium

APPENDIX 3. INTENSITY CURVES FOR PHENOTYPING

Figure: Intensity curves for cell categories phenotyped in QuPath. The density of the marker present in each cell category is seen on the y-axis. The intensity of the marker is seen on the x-axis. For example, to phenotype regulatory T lymphocytes, the intensity threshold is set at the boundary where FOXP3 is only present in the T-helper category, which is at 150.

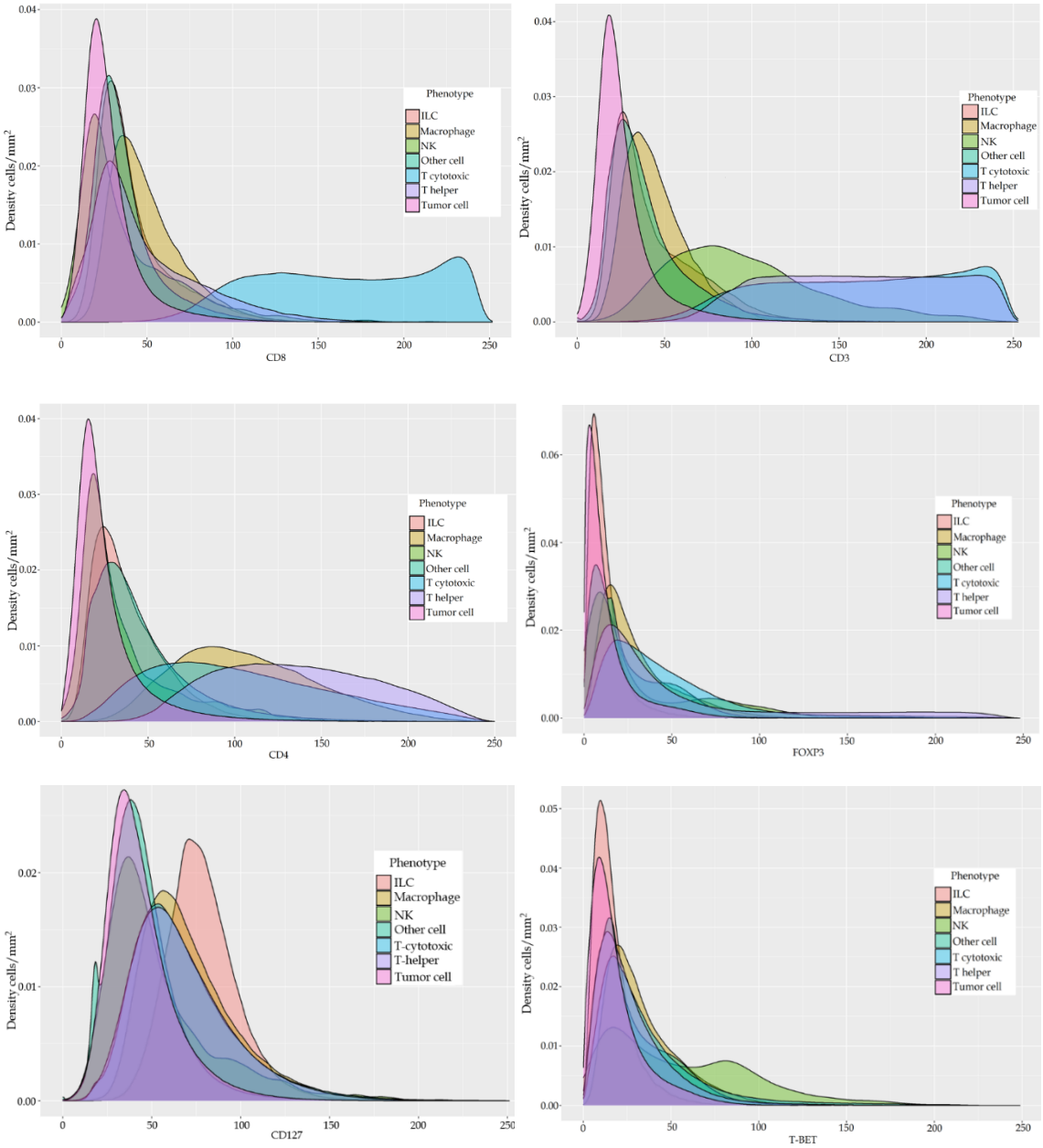

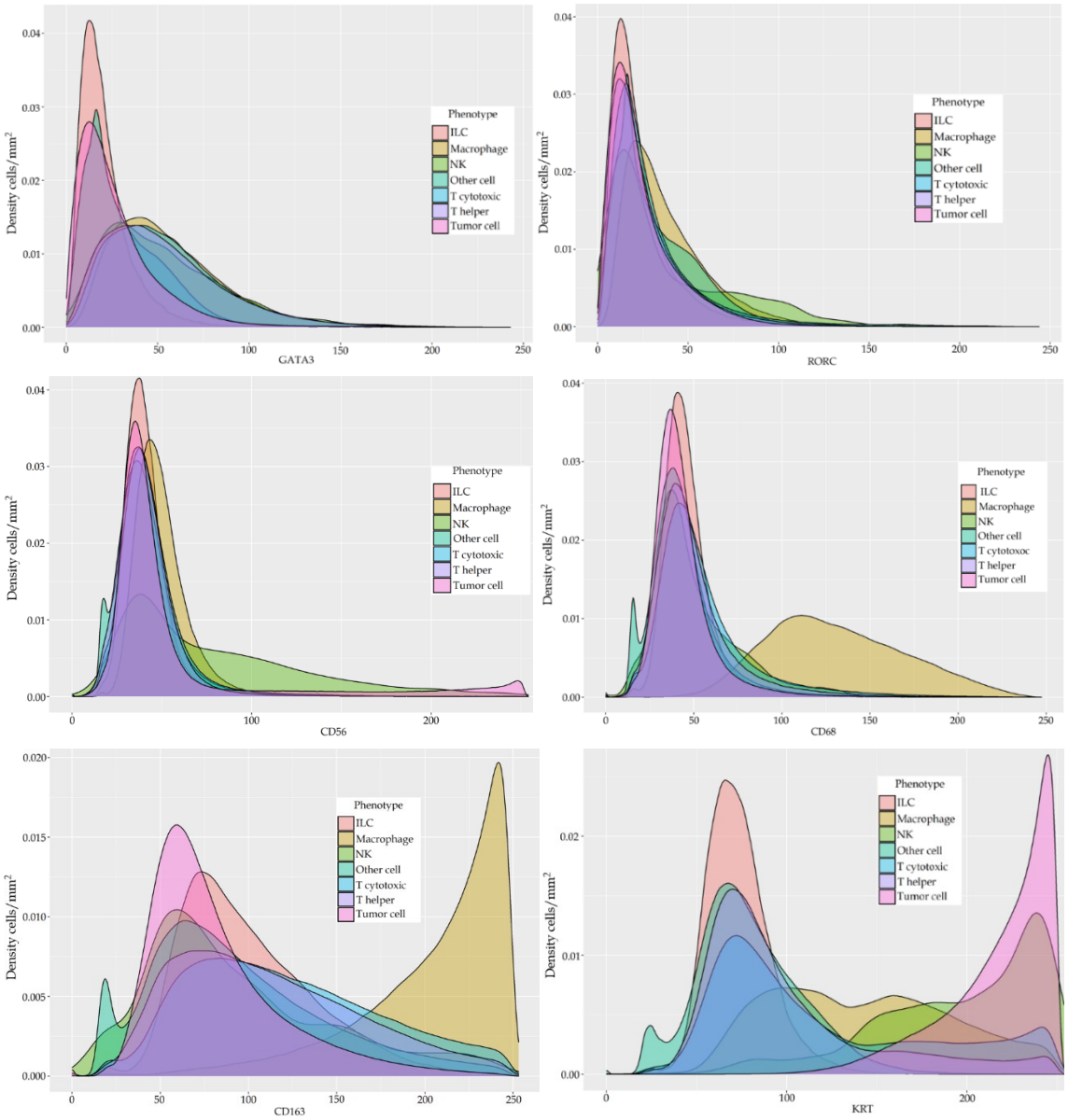
Density cells/mm²
GATA3
RORC
CD56
CD68
CD163
KRT
Phenotype
ILC
Macrophage
NK
Other cell
T cytotoxic
T helper
Tumor cell

APPENDIX 4. ROC-CUTOFFS

TABLE: The used ROC-cutoffs for Kaplan-Meier survival curves three and five years post-operation.

Cell density (cells/mm^2)	**Th1**	**Th2**	**Th17**
Tumor CT	21,420	50,642	5,380
Stroma CT	42,463	269,337	19,714
Overall CT	20,779	139,755	11,591
Tumor IM	19,857	71,022	10,831
Stroma IM	45,120	354,339	51,371
Overall IM	24,940	145,799	25,745

APPENDIX 5. MARKER STAIN INTENSITY

Figure: Marker stain intensity per TMA block.

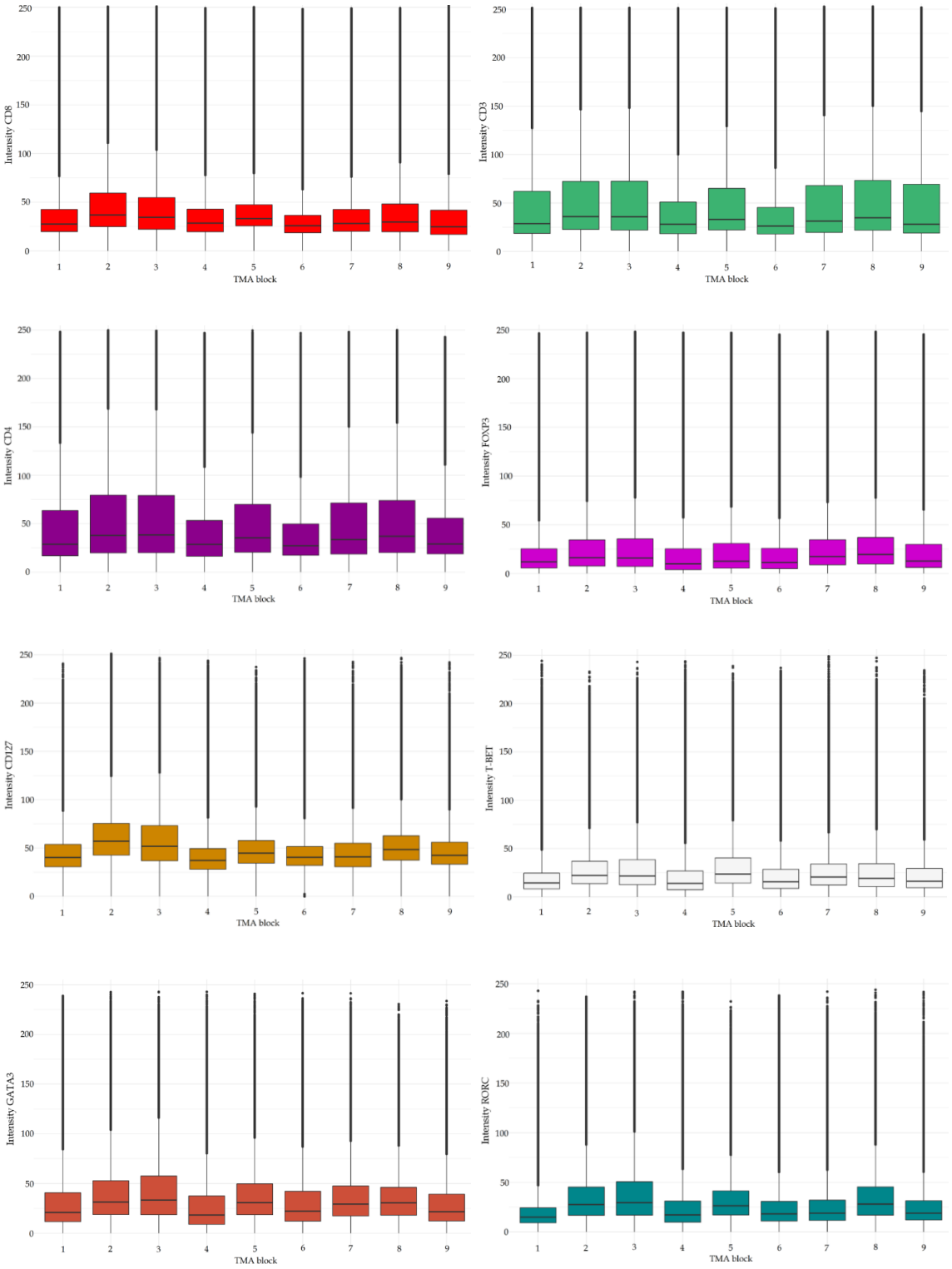

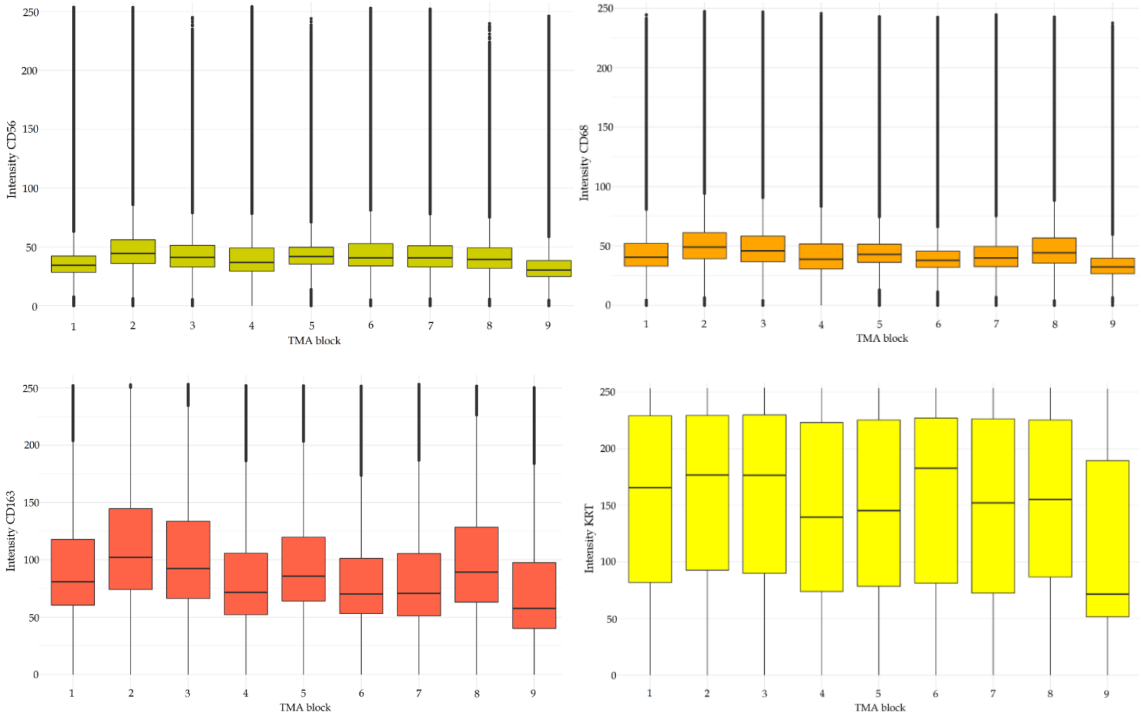
Intensity CD56
Intensity CD68
Intensity CD163
Intensity KRT
TMA block
0
50
100
150
200
250
1
2
3
4
5
6
7
8
9